Review

Contribution of Microwave Irradiation in the Synthesis of Inorganic Compounds: An Italian Approach

Cristina Leonelli *, Elena Colombini, Cecilia Mortalò *

Posted Date: 19 November 2025

doi: 10.20944/preprints202511.1382.v1

Keywords: microwave chemistry; hydrothermal microwave-assisted synthesis; microwave-assisted self-high temperature sustained synthesis; metastable phases; particle size homogeneity; oxides; composites; phosphates; zeolites; high entropy alloy

 doi:10.20944/preprints202511.1382.v1

Review

Contribution of Microwave Irradiation in the Synthesis of Inorganic Compounds: An Italian Approach

Cristina Leonelli [1,*] , Elena Colombini [1] and Cecilia Mortalò [2,*]

[1] Department of Engineering "Enzo Ferrari", University of Modena and Reggio Emilia, Via P. Vivarelli 10, 41125 Modena, Italy

[2] Institute of Chemistry and Condensed Matter and Technologies for Energy (ICMATE), National Research Council (CNR), Corso Stati Uniti 4, 35127 Padova, Italy

* Correspondence: cristina.leonelli@unimore.it; cecilia.mortalo@cnr.it

Abstract

Microwave heating has a good number of advantages in the synthesis of inorganic compounds when opportunely exploited. A deep knowledge of the interaction of the electromagnetic waves and matter is necessary to optimize irradiation of the reactor vessel so that to obtain homogeneous heating for homogeneous nucleation and growth of particle, localized heating of starting self-sustained high temperature synthesis and generate superfast heating and cooling profile to get metastable crystals. Case studies of pure oxides, mixed oxides, composites, phosphates, zeolites, and high entropy alloys have been discussed in the international frame of the academic and industrial research covering the last 20 years of microwave chemistry where Italian researchers covered a relevant role.

Keywords: microwave chemistry; hydrothermal microwave-assisted synthesis; microwave-assisted self-high temperature sustained synthesis; metastable phases; particle size homogeneity; oxides; composites; phosphates; zeolites; high entropy alloy

1. Microwaves Interaction with Matter

Microwaves (300 to approximately 300,000 MHz) could be regarded as a potent energy source as opposed to a heat source. In order to effectively apply microwave energy to any synthetic route, it is essential to identify the appropriate tools and knowledge in the optics of electromagnetic waves [1–5].

Molecular rotations and ionic species movements can be activated by the low energy carried by microwaves. These are non-ionizing waves with an energy interval of approximately $1.2*10^{-6}$ - $1.2*10^{-3}$ eV ($2.86*10^{-5}$ – 0.286 kcal/mole), corresponding to a frequency of 300 MHz-300 GHz (Table 1). By contrast, the typical covalent bond has an energy of around 2 to 5 eV (46-115 kcal/mole), and a hydrogen bridging bond has an energy of 0.2 eV [6]. Inducing chemical reactions by cleaving molecular bonds is only possible by employing higher-energy irradiation (e.g. UV or visible light, which is used for photochemistry). Therefore, it is clear why microwaves have been classified as '*non-ionizing radiation*'.

In dielectric media, such as water and aqueous solutions, when microwaves couple directly with the molecules provoking electric dipole rotation or periodic movement of charge carriers (contribution known as "ionic conduction") [10,11].

 doi:10.20944/preprints202511.1382.v1

Table 1. Features of microwaves at different microwave frequencies used worldwide. [adapted from Refs: 7-9].

Frequency range	Energy Range (eV)	Penetration depth in water[1]
300 MHz-300 GHz	$1.24*10^{-6}$ - $1.24*10^{-3}$	30 cm - 1 mm
2450 MHz (used worldwide)	$1.01*10^{-5}$	12.25 cm
5800 MHz (used worldwide)	$2.40*10^{-5}$	1.00 cm

[1] Calculation for water at 25°C.

These are the two fundamental mechanisms by which microwaves transfer energy to a substance, which is then heated by "molecular friction." Similar mechanisms are active for magnetic media and extend to magnetic dipoles. This type of energy transfer, also known as "microwave absorption," leads to a rapid rise in temperature when microwaves are turned on. Thus, it can be described as "instant on-instant off," offering easy reaction control. When the microwaves are turned off, only latent heat remains in the reaction vessel, which has cold walls and a hot reactant volume (Figure 1). In this context, the temperature profile is inverted compared to radiant heating, which typically heats the reactor walls to transfer heat to the reactant volume [12].

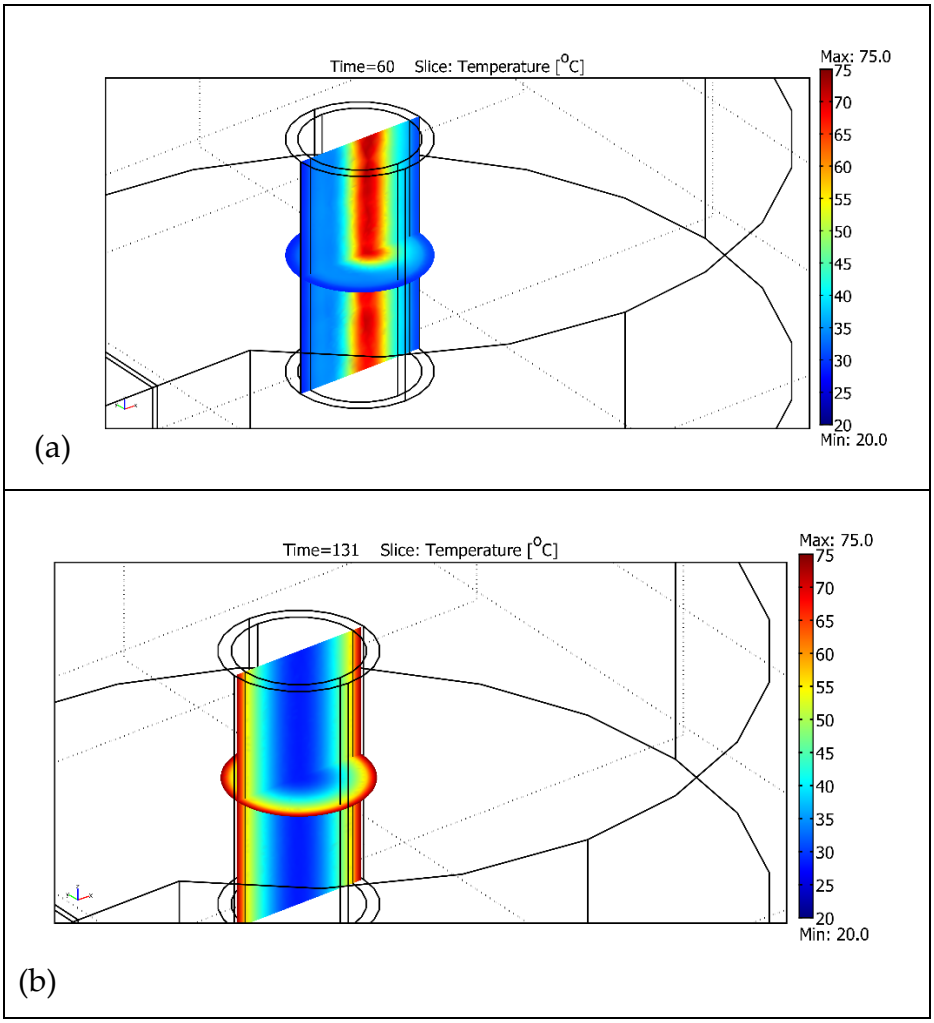

Figure 1. In a cold environment, matter absorbs electromagnetic radiation. Therefore, an object heated by microwaves cools down due to the surrounding cold air. This results in an inverted temperature profile compared to hot air, oil bath, or gas heating methods as visible from the reactor vessel heated with MW irradiation (a) and with conventional radiant heating (b).

To conclude the short description of general microwaves/matter interaction, we should stress the importance of the "*penetration depth*", *dp*. When the electromagnetic field, EMF, is dissipated in the reactant volume as dipole rotation, electromagnetic energy is absorbed. Therefore, the distance

 doi:10.20944/preprints202511.1382.v1

that the field can penetrate the body diminishes according to the absorption efficacy. The relative penetration depth is defined as the point in the reactant at which the EMF reaches approximately 37% of its output amplitude (Figure 2). The penetration depth is inversely related to the frequency of the excitation; higher frequencies result in lower penetration depths (Table 1).

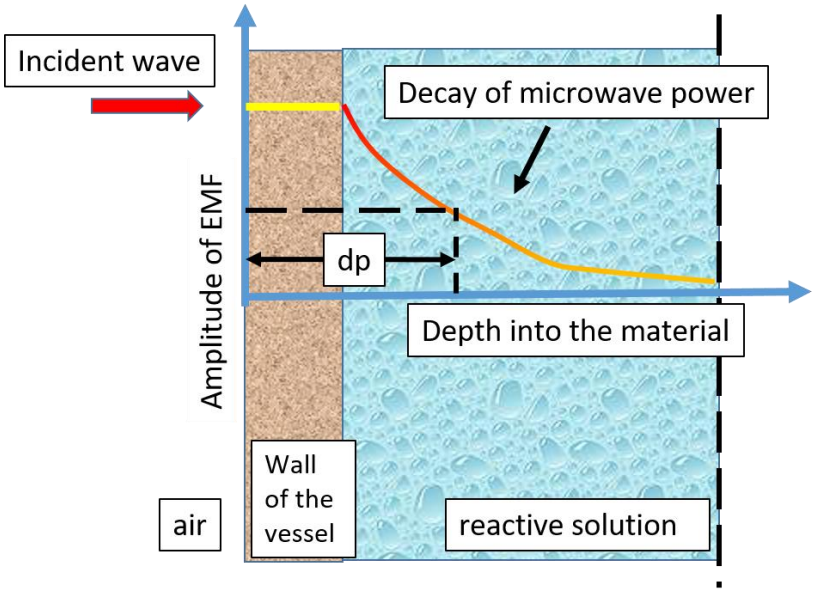

Figure 2. The absorption of electromagnetic radiation incident on the vessel wall and the reactive solution. Assuming that the vessel wall is perfectly transparent, the incident wave propagates without losing energy. The reactive solution absorbs microwave energy, as indicated by the decay of its amplitude.

However, the absolute depth of penetration - i.e. how deep the field can penetrate into the body - also depends on the output field strength or amplitude of the electromagnetic field-EMF (Figure 2). Another relevant feature of the absorption of electromagnetic energy by matter is that the absolute depth of penetration is generally larger when the material does not absorb electromagnetic energy, i.e., when it is transparent to microwave passage, as in the case of reaction vessels (Table 2). Using the most transparent material to contain the reactant mixture at the proper reaction temperature reduces energy loss through the vessel wall.

Table 2. Penetration depth in different media calculated for microwave irradiation at the frequency of 2450 MHz and at a temperature of 25°C. adapted from Ref. [1].

Material	Penetration depth (cm)
Metallic plate (Al, Cu, Ag, Stainless steel, ….)	$1\text{-}8x10^{-4}$
Distilled water	1.68
Tap water	1.25
ice*	1100
Hollow glass	35
Porcelain	56
Epoxy resin	4100
Teflon	9200
Quartz glass	16,000

*value measured at -12°C.

2. Microwaves and Chemical Reactions

 doi:10.20944/preprints202511.1382.v1

During microwave irradiation at the frequency most commonly adopted by chemical reactor producers, i.e. 2.45 GHz or 2450 MHz, electromagnetic waves transfer energy every 10^{-9} seconds per cycle (one cycle per second is one hertz). Kinetic molecular relaxation from this energy occurs in approximately 10^{-5} seconds. Thus, the energy transfers faster than the molecules can relax. This results in a non-equilibrium state with high instantaneous temperatures, which affects the system's kinetics. The most evident effect of these extremely fast heating processes is "*solvent superheating*", which is when the registered boiling temperature is higher than the conventionally measured one by 2 to 6 °C. [13].

In addition, some chemical moieties, such as stronger dipoles, are more sensitive to the microwave field than others. Therefore, it is possible to preferentially heat some reactants within a mixture of reactants while keeping the temperature of others lower. This specific feature of microwave heating has been used to promote regio-, chemo-, and stereo-selectivity [14–17].

For many years, errors in temperature measurement during microwave irradiation, along with the aforementioned features, have led many scientists to believe that the non-thermal effects of microwave heating are responsible for the many beneficial effects observed in microwave-assisted chemical synthesis [18–21]. Nowadays, most researchers who apply microwave irradiation to chemical synthesis agree that there is little to no hard evidence of specific or non-thermal microwave effects. Any such effects observed in the literature are likely due to irregularities in temperature measurement. Therefore, we can conclude that accelerating synthetic processes involves applying Arrhenius's law: doubling the reaction temperature halves the reaction time (Figure 3).

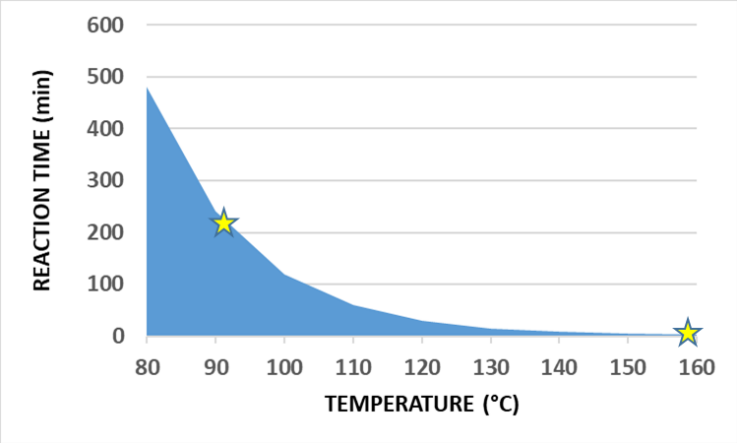

Figure 3. A reaction that is performed in boiling ethanol (approx. 90 °C) within 4 hours can be performed at 160 °C in approximately 2 minutes.

Temperature measurements remain an unsolved problem, which is further complicated by the endo- or exothermic effects of individual reactions. If we consider the microwave source the primary source of energy and the enthalpy of the reaction the secondary source of heating, then we can observe features that have not always been carefully investigated. Specifically, the microwave source can operate in continuous or intermittent scenarios. In the former, the power of the electromagnetic radiation is continuously modulated, typically from a few watts to 1000 or 1500 W. In the latter, the microwave source uses an output power equal to the maximum set value in the ON position and cycles off in the OFF position. The most advanced microwave reactors typically use the continuous regime, which results in a temperature increase in the reaction vessel proportional to the emitted power of the microwave radiation (Figure 4). When the reaction begins, the enthalpy sum increases or decreases the value perceptible by the temperature sensor depending on whether it is an exothermic or endothermic reaction. In the case of an exothermic reaction, the microwave emitter's power decreases and may even reach zero, as in highly exothermic reactions such as self-combustion

 doi:10.20944/preprints202511.1382.v1

synthesis. It is inappropriate to speak of MW-assisted synthesis in these cases. However, the definition of MW-ignited synthesis is appropriate [22].

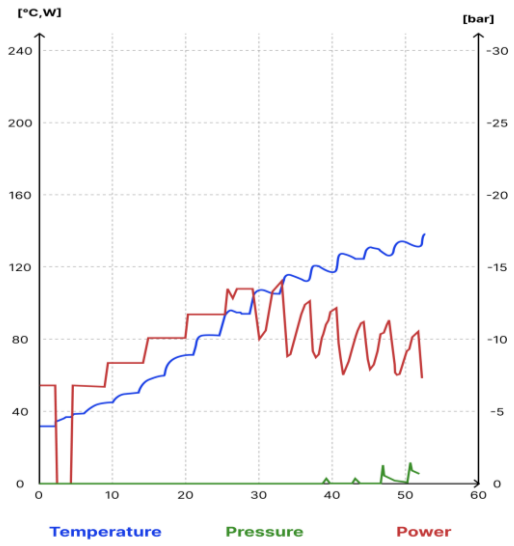

Figure 4. Temperature, microwave emitted power and pressure recorded in a pressurized reaction vessel during a chemical reaction. After about 30 min from the beginning of the experiment, the exothermic reaction increases the temperature while microwave power is lowered with the goal to maintain a constant heating rate till the scheduled temperature of 140°C. [Data specifically collected for this article].

3. Microwave in Inorganic Chemistry

Summarizing what described in Section 2., microwave irradiation results in energy-efficient internal heating through the direct coupling of microwave energy with dipoles and/or ions present in the reaction mixture. The faster reorientation of polar water molecules produces friction between them and generates internal heat. The amount of internally generated heat depends on the microwave power level, frequency, sample size, moisture content and the dielectric loss factor of the product. We should consider the penetration depth of microwaves within the reaction mixture and use the correct vessel geometry and (almost) microwave-transparent vessel walls to efficiently heat the mixture on a molecular level through direct interaction with the molecules (solvents, reagents, catalysts, etc.). Due to the direct 'in-core' heating (i.e. no initial heating of the vessel surface), the temperature gradient resulting from microwave irradiation is inverted compared to that of a conventionally heated system (see Figure 1).

These features have been exploited in inorganic synthesis since Komarneni and Roy's pioneering study in 1985 [23,24], where classical chemical reactions often take a long time and are energy inefficient, especially in hydro- or solvo-thermal environments or in solid state reactions or crystallization processes [25]. In the pressurized vessel, developed also for analytical purposes by several manufacturers, the MW transparent wall of the reactor ensures efficient energy transfer from MW to reactant, resulting in fast heating that has never been recorded in classical conditions. In 1992, Komarneni coined the term “microwave-hydrothermal (M-H)” for reactions performed at temperatures above the boiling point of water or other solvents and pressures greater than 1 atm [26].

Many inorganic materials are known to strongly couple to microwaves at ordinary temperatures meaning that they efficiently will heat up in a microwave irradiated environment. The same is true for the polar solvents used in the reactant mixture [27]. As mentioned above, the energy efficiency and heat dissipation in microwave applications are determined by the specimen’s dielectric properties, while the energy conversion rate is influenced by reaction time and temperature [2]. When reactants do not absorb microwave energy, as with polar molecules, adding a material that can absorb microwave energy and transfer heat to the reactants is a solution known as a microwave hybrid

 doi:10.20944/preprints202511.1382.v1

heating (MHH) [28]. This well-established technique is used in organic synthesis, where a solid absorber—typically silicon carbide (SiC) or magnetic compounds, such as susceptor powders—heats the reaction mixture and provides fast kinetics by reducing reaction time in non-aqueous environments [29]. In MHH, the most important factor is selecting materials for absorbance and insulation to avoid contamination [30].

When non-conductive inorganic materials are heated by microwave-induced dielectric loss in solvent-free conditions, it is important to adopt a convenient experimental setup to prevent heat loss and homogeneize the temperature profile within the reactive solid mixture. The most common method involves embedding pellets of reactant powders in the same mixture and surrounding it with glass wool to prevent heat loss from the reaction mixture [31].

Over the years, researchers have achieved many advantages through the unique features of microwave heating:

- rapid heating to temperature of reaction,
- increased reaction kinetics,
- elimination of metastable phases
- forming of novel phases
- high purity products
- uniform nanosized powder
- novel crystalline morphologies

These advantages have resulted in extraordinary new scientific developments in processing a variety of inorganic materials, such as carbides, nitrides, complex oxides, silicides, zeolites, apatite, semiconductors, and metal nanophases, including quantum dots, nanowires, nanorods, and nanobelts.

The Italian contribution to inorganic chemistry has been relevant also in the search for proofs of the above mentioned non-thermal effect. In particular, the observation of some of the authors of this article around the years 2010-2015 on the homogeneity of nanopowders production during hydrothermal synthesis of pure oxides was interpreted as pure thermal effect [25,32,33]. Microwave-assisted reactions are more selective than conventionally heated reactions and produce narrower particle size distribution curves thanks to a narrower temperature range (Figure 5). This has also been confirmed for solvothermal syntheses: the homogeneity of particle size was detected only when the reaction vessel was twice the size (or smaller) than the penetration depth [34].

In the following section, we present the results of Italian research groups' application of microwave chemistry to inorganic synthesis in liquid and solid state processes over the last 20 years. Our goal is to provide readers with a diverse overview of applications at the forefront of inorganic materials chemistry.

We would like to inform the reader that we have intentionally left out the synthesis of nanoparticles, which are mostly used for catalytic applications, as their main application field might require a more focused review article.

 doi:10.20944/preprints202511.1382.v1

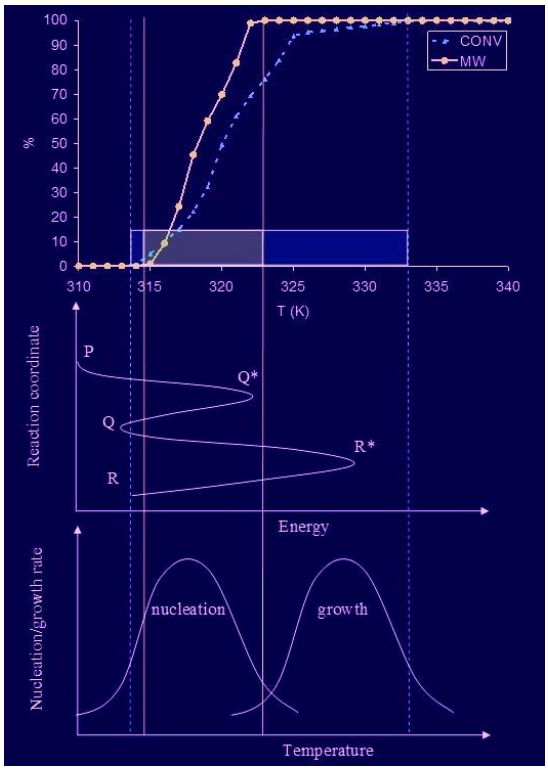

Figure 5. The cumulative temperature distribution in microwave heating (blue curve in upper plot) results in a much narrower range than conventional heating (red curve in upper plot) and is compared with the reaction profile (middle plot) and illustration of nucleation and growth rate curves (bottom plot. The overall temperature increase within the reaction vessel covers the conventional heating range (314-333 K), indicated in red, and the MW heating range (315-323 K), indicated in blue. In the MW heating case, the system temperatures and energies are such that only product Q is formed. In the conventional heating case, the broader temperature distribution leads to the formation of products Q and R. adapted from Ref. [33].

4. Pure Oxides

Four main synthesis routes for metal oxide preparation are: the solid state reaction route, the sol-gel, the combustion route, and the precipitation route [35]. In addition, the solvothermal and hydrothermal methods are also used [36]. Microwave-assisted methods have emerged as a highly effective approach for the controlled synthesis of different metal oxides offering distinct advantages in terms of reaction kinetics, phase purity and morphological control. The rapid, volumetric heating characteristic of microwave irradiation enables homogeneous nucleation, shorter reaction times and greater crystallinity than can be achieved using conventional thermal treatments. Several contributions from Italian research groups have provided valuable insights into the versatility of microwave-assisted synthesis strategies for zinc oxide (ZnO), titanium oxide (TiO_2), cerium oxide (CeO_2) and derivatives (doped-CeO_2), iron oxides (Fe_2O_3, Fe_3O_4), ZrO_2-based oxides and others (i.e. CdO, SnO_2, SiO_2).

4.1. ZnO

Chemoresistive devices based on Pure-Zinc Oxide (ZnO) and doped-ZnO nanostructures materials were prepared by Trocino et al. by a simple and fast microwave irradiation method [37].

Pure ZnO and Bi-doped ZnO nanoparticles with different dopant concentration were prepared by Prakash et al. using a microwave irradiation method [38]. The optical and photoluminescence properties of obtained samples were also investigated showing a decrease of the band gap energy (Eg) values with Bi doping level and a modification of the photoluminescence pattern, with promising potential for optical applications.

 doi:10.20944/preprints202511.1382.v1

Microwave assisted precipitation method was used by Gionco et al. for preparation of bare and N-doped nanostructured zinc oxide, as potential highly efficient photocatalysts for the degradation of phenol and 2,4-dichlorophenol under UV-A and visible light irradiation [39].

Uniform and highly crystalline ZnO nanoparticles were synthesized using an innovative microwave-assisted solvothermal synthesis by Garino et al. [40,41]. Highly-crystalline, round-shaped ZnO nanocrystals of 20 nm in diameter were obtained, optimized for use in biological applications. ZnO nanocrystals showed great biocompatibility towards pre-osteoblast cells and promising antimicrobial activity against E. coli and S. aureus. Compared to powders prepared by the traditional conventional solvothermal approach, the microwave-assisted ZnO NCs exhibited enhanced colloidal stability in both ethanol and water, maintaining their dispersion over extended storage times. Their more uniform size, shape and surface chemistry, combined with this long-term colloidal stability, ensures highly reproducible biocompatibility data, making the microwave-assisted process particularly advantageous for bio-related studies.

Similarly, Gautier et al. compared the classical thermal decomposition route with a microwave-assisted approach for synthesising ZnO nanoparticles, highlighting the superior efficiency and sustainability of the latter [42]. Microwave irradiation enabled the rapid formation of well-crystallised ZnO particles measuring ≈37–45 nm within a few minutes. This yielded materials with a surface area and pore volume nearly double that of materials obtained by the conventional method. Using coadjutants such as melamine and wine waste extracts improved dispersion and textural properties further, and the microwave process promoted the formation of carbon nitride species. This slightly affected the ZnO band gap, suggesting enhanced photocatalytic potential. Overall, this study reinforces the role of microwave-assisted synthesis as a green and versatile tool for producing nanomaterials with tailored structural and functional properties.

4.2. CeO_2

In two comparative studies by Natile, Glisenti and co-workers, nanostructured CeO_2 powders were synthesized via microwave-assisted hydrolysis and conventional precipitation methods, followed by thermal treatments at different temperatures [43,44]. Microwave-assisted synthesis produced smaller particles (3.3–4.0 nm) with a narrower size distribution, a greater surface area (72 m^2/g) and a higher concentration of acidic and basic surface sites than conventionally prepared samples. Moreover, CeO_2 obtained by microwave treatment exhibited higher surface reducibility and enhanced reactivity towards methanol oxidation, even at room temperature, producing formate and carboxylate species more efficiently than conventionally synthesised samples. These findings demonstrate that microwave irradiation enables rapid and uniform heating, which promotes simultaneous nucleation and reduced agglomeration, thereby enhancing both structural and surface catalytic properties of CeO_2.

In the study by Bonamartini Corradi et al. [45], nanocrystalline CeO_2 powders were successfully synthesized using a microwave–hydrothermal method, achieving high crystallinity in just 5 minutes at 13.4 atm. Compared to conventional hydrothermal approaches, which typically require 4–40 hours, this method provides a ~50-fold reduction in reaction time while delivering comparable structural and morphological properties. Furthermore, the process permitted the use of more concentrated precursor solutions, enabling scalable synthesis (up to ~160 g/L) without compromising powder quality. These results clearly demonstrate the significant advantages of microwave-assisted hydrothermal synthesis in terms of time efficiency, scalability, and control over particle characteristics.

Gondolini et al. developed a new method for synthesizing nanocrystalline gadolinia-doped ceria (GDC) powders using a microwave-assisted polyol process [46]. GDC powders were produced by heating a diethylene glycol solution of cerium and gadolinium nitrate precursors in a microwave oven at 170°C for 2 hours, bypassing the need for an additional calcination step, which typically causes severe aggregation and sintering in other chemical methods. The resulting GDC powder

 doi:10.20944/preprints202511.1382.v1

demonstrated good sinterability and exhibited ionic conductivity comparable to commercial nanometric GDC, making it a promising material for IT-SOFC electrolyte applications.

The same authors optimized a successful method for the synthesis of nanocrystalline CeO_2 particles with controlled morphology using a simple one-step microwave-assisted method [47]. By adjusting the reaction temperature, the authors were able to tune the crystal structure and morphology of the CeO_2, obtaining either pure nanocrystalline CeO_2 or a mixture of CeO_2 and cerium formate phases. The microwave heating led to the rapid and homogeneous nucleation of the CeO_2 particles, allowing for the formation of complex morphologies like flowerlike and needle-like shapes. The CeO_2 powders with the complex morphologies exhibited enhanced catalytic activity for the total oxidation of toluene compared to other samples, highlighting the benefits of this microwave-assisted synthesis approach.

More recently, in the study by Salusso et al. [48], a highly defective CeO_2 sample synthesized via microwave-assisted preparation was shown to host frustrated Lewis pairs (FLPs), which played a key role in the activation of CO_2 and methanol toward monomethylcarbonate (MMC) formation. Among several CeO_2 materials with varying defect and Ce^{3+} levels, the microwave-prepared sample exhibited both high Ce^{3+} content (>30%) and abundant surface defects—conditions essential for FLP formation. The study highlights that microwave synthesis can promote the formation of defect-rich, Ce^{3+}-enriched surfaces, enabling FLP generation and enhancing catalytic activity in CO_2 activation pathways that are not achievable with ceria prepared using conventional methods.

In the work by Ballauri et al., pure and Pr-doped ceria ($Ce_{90}Pr_{10}$) were synthesized using three different methods, including a microwave-assisted route that yielded nanostructured spherical particles [49]. While all synthesis approaches led to high surface area supports and comparable catalytic performances for Pd-based methane oxidation, the microwave-assisted method stands out for its reduced reaction time and synthetic efficiency, offering a rapid and effective route to produce highly dispersed, catalytically active materials.

4.3. TiO_2

Conciauro et al. reported the synthesis of anatase TiO_2 explored as additives for aluminosilicate bricks [50]. Powders having two different morphologies were obtained via microwave-assisted procedures, which provided fine control over particle size and shape and avoided the need for post-calcination. The uniform heating promoted by microwave irradiation ensured the formation of highly homogeneous nanocrystals. When incorporated into aluminosilicate refractories (0.5–2 wt%), these microwave-derived nanoparticles led to improvements in both mechanical strength and thermal insulation. The enhanced performance was correlated with the increased porosity induced by the microwave-synthesized nanophases, highlighting their role in tuning the microstructural and functional properties of ceramic matrices.

Microwave irradiation was employed by Zhang et al. to anchor TiO_2 nanoparticles onto carbon supports, such as reduced graphene oxide (RGO) and amorphous carbon [51]. The fast and uniform heating achieved by microwaves enhanced the interfacial coupling between TiO_2 and the carbon substrate, producing smaller nanoparticles with narrower size distributions and improved dispersion. This stronger TiO_2-carbon interaction resulted in superior photocatalytic efficiency, demonstrating that microwave-assisted synthesis can effectively modify the surface chemistry and nanostructure of TiO_2-based hybrid materials.

Filippo et al. developed a rapid and simple method for preparing pure anatase titania nanoparticles using a non-aqueous, microwave-based approach [52]. The resulting nanopowders had a large specific surface area and an elongated morphology, with lengths of 13.8 ± 5.5 nm and diameters of 9.0 ± 1.2 nm. They showed excellent Rhodamine B performance compared to both commercial spherical nanotitania P25 and P25 loaded with platinum.

The same authors developed a two-step, similar method for producing TiO_2-polyvinyl alcohol (PVA) hybrid nanoparticles that exhibit enhanced photocatalytic activity under visible light conditions [53]. Microwave heating facilitated the rapid nucleation and crystallisation of TiO_2, while

 doi:10.20944/preprints202511.1382.v1

subsequent PVA coating controlled aggregation and surface coverage. The hybrid with a TiO_2:PVA ratio of 1:0.050 exhibited the fastest Rhodamine B degradation rate, approximately 1.4 times faster than unmodified TiO_2. This enhanced performance was attributed to the effective interfacial charge separation promoted by the microwave-enabled synthesis and optimised polymer coverage.

Tian and Italian collaborators [54] synthesized (N,Fe)-codoped activated carbon/TiO_2 photocatalysts via a microwave-assisted sol–gel process. This achieved the rapid crystallization of mixed anatase–rutile phases (approximately 20 nm) that were uniformly dispersed on activated carbon. Microwave heating enabled the efficient incorporation of N and Fe dopants into the TiO_2 lattice, thereby narrowing the band gap to 2.58 eV and extending light absorption into the visible region. The resulting photocatalyst showed a high surface area (≈550 m^2 g^{-1}) and achieved 93% formaldehyde degradation under Xe-lamp irradiation, showing improved visible-light activity and recyclability.

Prato et al. optimized the synthesis of phase-pure rutile TiO_2 nanoparticles through a microwave-assisted hydrothermal approach [55]. Applying microwaves during hydrothermal treatment accelerated the crystallisation process and improved the structural order of rutile TiO_2. The resulting nanoparticles exhibited exceptional photocatalytic activity in the degradation of methyl orange in the presence of H_2O_2. EPR analysis revealed that microwave treatment favoured the generation of superoxide radicals ($O_2^{\bullet-}$), which are directly linked to the enhanced photoactivity. This highlights the influence of microwave-driven thermal processes on defect chemistry and redox behaviour.

More recently, in the study by Alfano et al., a one-step microwave-assisted synthesis was employed to produce a graphene/TiO_2 nanocomposite [56]. This nanocomposite was then used to fabricate a chemiresistive sensor for room-temperature ethanol detection. The microwave method allowed TiO_2 nanoparticles to be incorporated directly and efficiently onto graphene sheets, resulting in a material with promising sensing properties. The sensor exhibited selective and reproducible responses to ethanol within the 15–50 ppm range with minimal interference from water vapour. This work demonstrates how microwave-assisted synthesis provides a fast and effective route for preparing TiO_2-based composites with potential in gas sensing applications.

Paradisi et al. developed a microwave-assisted vacuum sol–gel process for the rapid and straightforward synthesis of crystalline TiO_2 nanopowders with photocatalytic activity [57,58]. In this case, microwave heating under vacuum conditions enabled rapid solvent removal and uniform energy distribution, leading to high-purity nanocrystalline TiO_2 with dispersibility and photocatalytic activity comparable to commercial powders. These microwave-synthesized TiO_2 nanoparticles have also been successfully embedded in sodium alginate matrices to prepare flexible and homogeneous bio-composite films for packaging and life science applications [59].

The same authors later investigated the microwave-assisted calcination of N-doped TiO_2 precursors [60,61]. Their studies demonstrated that the crucible material strongly influenced the resulting crystalline phase: porcelain crucibles yielded mixed phases, whereas quartz fiber crucibles produced pure rutile at only 250 °C. Although this outcome was attributed to thermal rather than specific microwave effects, it nonetheless highlights the capacity of microwave-assisted heating to precisely modulate thermal transformations during TiO_2 processing. Efficient B-doping in TiO_2 was also reported by Carlucci et al. where TiO_2:(B) nanocrystals of anatase were prepared in a single, fast reaction step (with a reaction time of about 45 minutes) using a microwave-assisted method. This method allows one to control the doping level and improves the performance of commercial titania in photocatalytic tests under visible light [62].

4.4. Iron Oxides

Spepi et al. [63] developed a microwave-assisted solvothermal synthesis method for producing superparamagnetic iron oxide nanoparticles (IONs), using a custom-made coaxial microwave antenna inside a pressurised reactor. This configuration enabled a homogeneous electromagnetic field to be distributed, thus avoiding the hot spots that are typical of conventional oven-type systems,

 doi:10.20944/preprints202511.1382.v1

while also allowing precise control of the temperature and pressure. Uniform maghemite nanoparticles (approximately 6 nm in size) with a narrow size distribution and a saturation magnetisation of up to 68 emu g^{-1} were obtained in just 5–15 minutes. The coaxial setup provided efficient, scalable and reproducible microwave heating, yielding high-quality IONs that are suitable for magnetic and biomedical applications.

In the study by Muhyuddin and Italian co-workers, microwave-assisted pyrolysis (MAP) was used to convert scrap tires into carbonaceous char for the sustainable synthesis of Fe–N–C electrocatalysts [64]. Microwave irradiation enabled rapid, uniform, and energy-efficient heating, enhancing carbon activation and promoting the formation of a porous, graphitically disordered matrix. This efficient energy transfer facilitated the uniform incorporation of Fe and N species, leading to Fe_3O_4 nanoparticles well-dispersed within the carbon framework. The resulting catalysts exhibited excellent ORR activity across acidic, neutral, and alkaline media, highlighting the effectiveness of microwave-assisted processing in coupling waste valorization with precise structural and functional control.

In their study, Porru et al. demonstrated that the microwave-assisted polyol method is a powerful and sustainable approach for the controlled synthesis of manganese- and zinc-doped iron oxide nanoparticles [65]. Microwave irradiation enabled rapid, homogeneous and energy-efficient heating of the polyol medium (diethylene glycol or tetraethylene glycol), resulting in excellent control over nucleation and crystal growth. This uniform energy distribution minimised the temperature gradients typically observed in conventional heating processes, resulting in highly reproducible nanoparticles with narrow size distributions and tunable morpho-structural features. The microwave-assisted process also enabled the precise incorporation of dopant ions (Mn^{2+} and Zn^{2+}) into the spinel lattice, strongly influencing both particle size and magnetic behaviour. Notably, despite their reduced crystal dimensions (approximately 10–15 nm), the nanoparticles exhibited exceptionally high saturation magnetisation values (above 90 emu/g), which can be attributed to the efficient energy transfer and rapid kinetics promoted by microwave irradiation.

Saladino et al. have developed a range of versatile, microwave-assisted strategies for synthesising superparamagnetic iron oxide nanoparticles (SPIONs) and nanoclusters for use in biomedicine and as antibacterial agents. Using hydrothermal or solvothermal microwave-assisted methods, SPIONs were functionalised with sugar ligands, citrate or L-lysine, yielding uniform nanoparticles (4–20 nm) and larger nanoclusters (up to 400 nm) with enhanced magnetic properties, surface charge and colloidal stability [66–68]. Selected SPIONs were further coated with fluorophore-doped silica or assembled into biofunctional hybrid microspheres via click chemistry. This enables combined applications in magnetic hyperthermia, fluorescence imaging, antibacterial activity, drug delivery and pollutant removal while maintaining a tunable magnetic response and reusability.

Mekseriwattana and Italian co-workers recently developed a microwave-assisted method for the rapid, shape-controlled synthesis of iron oxide nanocubes (IONCs), achieving iron conversion yields of up to 80% [69]. The efficient volumetric heating provided by microwaves enables nucleation and growth to occur within minutes, and benzaldehyde acts as a key shape-directing agent, enabling control of the size to be achieved between 13 and 30 nm (Figure 6). The resulting, highly crystalline superparamagnetic IONCs exhibit a saturation magnetization of over 80 emu·g^{-1} and excellent SAR values of up to 400 W·gFe^{-1} under clinical magnetic field conditions.

 doi:10.20944/preprints202511.1382.v1

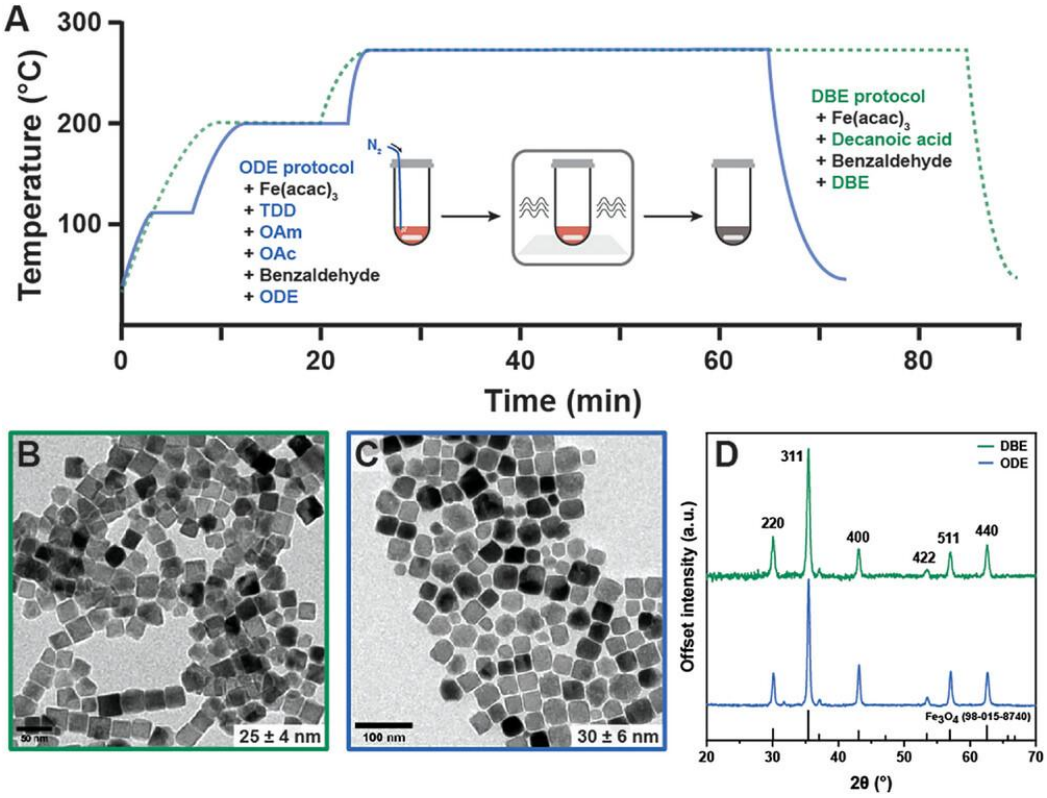

Figure 6. A) Synthesis scheme and the temperature profile of the MW-assisted synthesis of the IONCs. Green and blue lines represent the temperature profiles of DBE and ODE protocol, respectively. B, C) BF-TEM image of the IONCs synthesized with DBE (framed in green) and ODE (framed in blue) protocols, respectively. D) XRD spectra of the corresponding IONCs samples. Black lines represent the theoretical peaks of Fe_3O_4 crystal (JCPDS card no. 98-015-8740). Adapted from Ref. [69].

Calsolaro *et al.* reported a microwave–ultrasound-assisted protocol for the rapid synthesis of hydrophilic and negatively charged iron oxide magnetic nanoparticles (MNPs) with tunable surface coatings [70]. The combined use of microwave and ultrasound irradiation enabled efficient control over particle size, morphology, and surface properties, yielding highly stable and dispersible MNPs. Among the tested coatings, an amino citrate–modified β-cyclodextrin provided amphoteric behavior, excellent cytocompatibility, and favorable NMR relaxometric performance, highlighting the potential of these MW/US-assisted MNPs for future MRI and theranostic applications.

4.5. ZrO_2-Based Oxides

The microwave-assisted hydrothermal synthesis is a widely used method for preparing zirconia and doped zirconia nanoparticles. Bondioli et al. [71] first reported the production of nanosized ZrO_2 powders by adding NaOH to an aqueous zirconyl chloride solution under microwave-hydrothermal conditions at 200 °C. This process yielded tetragonal ZrO_2 with very fine particle sizes (10–20 nm), a narrow size distribution and good chemical homogeneity, thus demonstrating the advantages of rapid and uniform heating. The same group later extended this approach to praseodymium-doped zirconia systems (0–10 mol% Pr), demonstrating that microwave-hydrothermal treatment under controlled temperature and pressure (up to 8 MPa) can form highly crystalline, stabilised tetragonal zirconia. Structural analyses confirmed that Pr atoms substituted for Zr in the lattice, forming homogeneous solid solutions while minimising amorphous content due to efficient, microwave-driven nucleation [72,73].

Building upon these pioneering studies, Rizzuti et al. applied the microwave-hydrothermal method to synthesise nanocrystalline zirconia from aqueous $ZrOCl_2{\cdot}8H_2O$ solutions [74]. The resulting powders consisted of primary nanoparticles measuring approximately 8 nm that

 doi:10.20944/preprints202511.1382.v1

aggregated into stable superstructures measuring 50–130 nm and remained dispersed for up to 15 days. The same authors subsequently investigated calcia-stabilised zirconia (CaSZ), which was obtained by irradiating a 0.5 M zirconyl chloride solution containing 6 mol% Ca^{2+} at 220 °C for 30 minutes [75]. This process produced tetragonal nanoparticles (~7 nm) with a narrow size distribution. Subsequent microwave-assisted sintering at 1300 °C for 5 minutes yielded dense ceramics with a uniform nanostructure and grain sizes between 90 and 170 nm, reaching 95% of the theoretical density.

More recently, Riva et al. investigated the effect of microwave hybrid heat treatment (MHH) on pre-sintered 3%mol yttria partially stabilized zirconia (3Y-PSZ) ceramics [76]. Treatments at 1200 °C for 5–15 minutes significantly reduced the monoclinic fraction in the first micrometres of the surface, achieving a thickness of less than 1 μm after 15 minutes. Grazing incidence X-ray diffraction enabled a precise mineralogical assessment to be made at different depths, confirming complete stabilisation in the tetragonal phase. Microwave treatment promoted densification with minimal grain growth and reduced open porosity to ~0.3%, demonstrating the advantage of volumetric heating in achieving uniform, fully stabilised 3Y-TZP microstructures in significantly less time than conventional sintering.

Giordana et al. [77] reported on a microwave-assisted sol-gel approach for preparing zirconia and sulphated zirconia (SZ) catalysts. This involved microwave-assisted gel drying, followed by microwave-assisted calcination using a susceptor to achieve homogeneous tetragonal ZrO_2 nanoparticles. Using microwaves drastically reduced the time and energy required for calcination, while preserving high crystallinity. The resulting SZ materials exhibited controlled surface acidity and demonstrated promising catalytic activity in the hydrolysis of glucose to 5-hydroxymethylfurfural.

4.6. Other Metal Oxides

Many other oxides have been prepared using microwave-assisted methods. For example, Corradi *et al.* developed a continuous-flow microwave-assisted hydrothermal process for the preparation of monodispersed silica nanoparticles using tetraethyl orthosilicate (TEOS) as precursor [78]. Varying the flow rate (43–101 mL min^{-1}) in a pressurized microwave reactor, enabled effective control of particle size and agglomeration, achieving spheres below 50 nm at higher flow rates. This approach shortened reaction times compared to conventional hydrothermal methods, highlighting the importance of flow control for process scalability.

A series of studies conducted by Neri and and colleagues further demonstrated the versatility of microwave-assisted synthesis for producing various functional metal oxide nanostructures with improved sensing performance. In their early work [79], the microwave irradiation was employed to synthesize various oxide nanostructures, including SnO_2, ZnO, $Cd(OH)_2$, and CdO. These were then deposited onto interdigitated alumina substrates to fabricate chemoresistive sensors. This study demonstrated that microwave-assisted processing enables rapid crystallization and fine morphological control, yielding nanostructured oxides with enhanced gas-sensing responses compared to those produced by conventional routes.

Building on this approach, well-defined hexagonal CdO nanosheets were also synthesized via a simple microwave-assisted chemical route [80]. The rapid and homogeneous heating promoted by microwaves facilitated the formation of crystalline CdO sheets with a controlled thickness (100–200 nm) and edge lengths of 1–3 μm. The resulting CdO-based chemoresistive sensors exhibited high sensitivity, fast response and recovery times, and excellent signal-to-noise ratios toward CO. These properties were attributed to the reduced agglomeration and improved gas diffusion achieved through microwave-assisted growth.

In a subsequent work, microwave-assisted synthesis of SnO_2 nanoparticles with controlled irradiation times were prepared, achieving crystalline cassiterite-type structures within only 5–15 minutes, without any post-annealing treatment [81]. Structural analyses confirmed that varying the irradiation time effectively tuned the crystallinity and morphology of particles. The resulting SnO_2

 doi:10.20944/preprints202511.1382.v1

sensors exhibited high ethanol sensitivity at temperatures below 100 °C, along with a peculiar inverted sensing response—an increase in resistance upon exposure to ethanol—attributed to surface interactions between ethanol's hydroxyl groups and oxygen vacancies. After annealing, conventional n-type behavior was restored, emphasizing the influence of surface chemistry and defect density on the sensing mechanism. This study further demonstrated the ability of microwave-assisted synthesis to tailor morphology, crystallinity, and surface states that govern gas–solid interactions in oxide-based sensors.

5. Mixed Oxides

5.1. Mixed Oxides and Perovskites

Bondioli et al. developed drying and firing microwave treatments for inorganic coprecipitated hydroxide gels, resulting in the successful extraction of a pink ceramic pigment belonging to the Al_2O_3/Cr_2O_3 oxide system [82]. Compared with pigments produced using conventional industrial ceramic methods, the introduction of microwave treatment can lead to a more continuous and efficient process that consumes a small fraction of the energy and time required for conventional treatment.

Bonometti et al. demonstrated the potential of microwave-assisted solid-state synthesis for rapidly preparing technologically relevant mixed oxides, such as chromites, ferrites, spinels and garnets [83]. This method produced pure phases such as Pb_2CrO_5, Na_2WO_4, YVO_4 and $Y_3Fe_5O_{12}$, often without the need for external susceptors, except for oxides that absorb poorly. In addition to being faster and more energy efficient, the MW method minimises contamination from crucible walls and improves yields, thus establishing microwaves as a powerful yet non-conventional tool for solid-state oxide synthesis.

Arbizzani *et al.* reported on the microwave-assisted, solid-state synthesis of $Ag_2V_4O_{11}$ (SVO), starting with V_2O_5 and Ag_2CO_3, using a single-mode microwave system featuring automated power control based on temperature feedback [84]. Microwave irradiation enabled SVO to be prepared rapidly in just 5 minutes at 250 °C, as opposed to 48 hours at 500 °C using conventional thermal synthesis. The resulting material exhibited structural and electrochemical properties that were fully comparable with those of thermally synthesised SVO.

Barison *et al.* [85] demonstrated the effectiveness of the microwave-assisted sol–gel Pechini (MWA-SGP) method in synthesising perovskite-type $BaCe_{0.65}Zr_{0.20}Y_{0.15}O_{3-\delta}$ powders. Compared to the conventional Pechini method, the microwave process significantly reduced the gelation and combustion steps from several days to a few hours, yielding high-purity nanocrystalline powders (120–200 nm) with improved sinterability and densities of up to 97% at 1400 °C. Building on this approach, the same authors synthesized $La_{0.80}Sr_{0.20}Ga_{0.83}Mg_{0.17}O_{3-\delta}$ electrolytes using both the conventional method and the MWA-SGP method [86]. This confirmed that microwave irradiation accelerates processing and enhances phase purity and ionic conductivity by 30–40%. These studies emphasise the potential of microwave-assisted Pechini routes for the rapid, cost-effective production of dense, single-phase perovskites with superior functional performance, making them particularly suitable for energy and electrochemical applications.

Ponzoni *et al.* [36,87,88] systematically investigated the microwave-assisted hydrothermal synthesis of $BiFeO_3$-based perovskites. In an earlier study [87], they optimised the influence of the precursor ratio, mineraliser concentration and temperature on $BiFeO_3$ formation, revealing that pure multiferroic BFO could be obtained within 30 minutes at 180–200 °C under controlled KOH concentrations (8–10 M). Microwave irradiation provided rapid, homogeneous heating, enabling precise control over nucleation and morphology and yielding submicrometric particles with tunable shapes. Building on this, the authors later extended the method to La-doped $Bi_{1-x}La_xFeO_3$ [88], achieving single-phase perovskite powders at 200 °C, which is a reduction in synthesis temperature of ~500 °C compared with conventional routes. These studies demonstrate how microwave

 doi:10.20944/preprints202511.1382.v1

hydrothermal processing can enable the ultrafast, low-cost fabrication of high-purity multiferroic and doped mixed-oxide perovskites.

Ruffo et al. investigated how non-magnetic Ca^{2+} and Mg^{2+} dopants influence the structural and magnetic properties of $GdFeO_3$ perovskite nanoparticles synthesized via various methods, including a microwave-assisted sol–gel process [89]. Microwave irradiation enabled rapid and homogeneous heating, promoting uniform nucleation and crystallisation, and producing more consistent results than conventional sol–gel and polyol methods. The microwave-assisted synthesis produced nanometric particles (20–45 nm) with solid-solution formation and consistent lattice parameters, while significantly reducing reaction time. While all methods produced similar compositions, the microwave-assisted approach improved structural uniformity and phase purity. This demonstrates its effectiveness in producing doped $GdFeO_3$ perovskites with tunable magnetic behaviour by precisely controlling energy input and reaction kinetics.

Wu and Italian colleagues [90] reported on the microwave-assisted synthesis of $BiVO_4$ with controlled morphology using surfactants such as sodium dodecyl benzene sulfonate (SDBS), polyvinylpyrrolidone (PVP) and ethylenediaminetetraacetic acid (EDTA). The presence of these surfactants directed the formation of octahedral, olive-like and hollow structures respectively, whereas the absence of surfactants produced irregular particles. Microwave irradiation (800 W, 100 °C for 3 hours) enabled rapid and uniform crystallization under atmospheric pressure, yielding well-defined morphologies. Subsequent CdS deposition via chemical bath produced $BiVO_4$-CdS Z-scheme photocatalysts with enhanced electron–hole separation. This study demonstrates that combining microwave-assisted routes with surfactant control enables the rapid preparation of nanostructured photocatalysts with tailored properties.

Mortalò et al. investigated the microwave-assisted sintering of Na-β′-Al_2O_3 powders using single-mode cavities at 2450 MHz, and preliminarily at 5800 MHz [91]. The single-mode setup enabled precise monitoring of surface temperature and forward power, facilitating the evaluation of energy efficiency. At 2450 MHz, isothermal treatment at 1300 °C for 40 minutes achieved ~90% densification, whereas pre-milling reduced this time to 10 minutes. At 5800 MHz, 92% densification was achieved in 3 minutes; however, thermal runaway and arcing limited process control. Dielectric measurements and numerical simulations provided insights into power density distribution and microstructural uniformity, which will guide the future optimisation of microwave sintering.

5.2. Composites

Dell'Agli *et al*. investigated the hydrothermal crystallization of coprecipitated Y-TZP/α-Al_2O_3 xerogels with 90 vol.% zirconia (3 mol% Y_2O_3) and 10 vol.% alumina [92]. The xerogels were treated under conventional (110 °C, 7 days) or microwave-assisted (250 °C, 2 h) hydrothermal conditions using different mineralizers. Microwave-assisted hydrothermal treatment enabled rapid crystallization, producing powders with low agglomeration, suitable for subsequent calcination to yield homogeneous t-ZrO_2/α-Al_2O_3 composites.

Barison *et al.* [93] reported on the synthesis of Ru/$La_{0.75}Sr_{0.25}Cr_{0.5}Mn_{0.5}O_3$-δ composites, in which Ru nanoparticles were deposited on the perovskite LSCM via microwave-assisted reduction. In this method, LSCM powder was ultrasonically dispersed in ethylene glycol, to which 5 wt.% of $RuCl_3 \cdot 0.8H_2O$ was then added. This dispersion was then irradiated in a microwave oven (Ethos D, 750 W for 1 minute) to allow the rapid and homogeneous reduction of Ru^{3+} and the nucleation of metallic Ru nanoparticles directly on the oxide surface. The resulting suspension was then washed with acetone and dried to yield a uniform distribution of 2–3 nm Ru particles. The fast, localised heating provided by microwaves ensured excellent metal dispersion and a strong metal–support interaction, thereby enhancing the catalytic activity and stability during propane reforming.

Neri *et al.* prepared SnO_2/reduced graphene oxide (RGO) nanocomposites through a one-pot microwave-assisted, non-aqueous sol–gel process [94]. This approach involved the simultaneous partial reduction of graphene oxide and formation of SnO_2 nanoparticles, yielding composites with uniform dispersion of oxide nanoparticles and tunable surface coverage. The fabricated SnO_2-RGO

 doi:10.20944/preprints202511.1382.v1

sensors exhibited excellent NO_2 sensitivity and selectivity, with responses that were highly dependent on the SnO_2/RGO ratio. This behaviour was linked to charge transfer processes at the n–SnO_2/p–RGO heterojunctions, highlighting the effectiveness of microwave synthesis in producing finely engineered hybrid sensing materials.

Tian et al. developed an efficient, microwave-assisted approach to rapidly synthesize activated carbon–titania (AC/TiO_2) nanocomposites with enhanced photocatalytic activity [95]. Microwave irradiation enabled the uniform deposition and crystallisation of anatase–rutile TiO_2 nanoparticles (20–50 nm) on the AC surface within 15 minutes at 700 W, resulting in a red-shifted optical absorption. The composite achieved 98% degradation efficiency of rhodamine B under UV light within 30 minutes. This superior performance was attributed to the synergistic effects of the mesoporous carbon support and the high TiO_2 content, which promote the formation of hydroxyl radicals (•OH).

Garino *et al.* reported on the synthesis of reduced graphene oxide (rGO)/Fe_2O_3 nanocomposites using a one-pot, microwave-assisted process [96]. This method is fast, eco-friendly and reliable for preparing ORR catalysts. Microwave irradiation reduced and functionalised the graphene oxide simultaneously, while promoting the uniform nucleation and dispersion of the Fe_2O_3 nanoparticles within the graphene matrix. The resulting nanocomposites exhibited well-dispersed nanometric iron oxide crystals and nitrogen functionalisation, leading to synergistic catalytic effects for the oxygen reduction reaction (ORR). This method allows the catalytic performance to be fine-tuned via the concentration of the precursor, producing materials whose electrochemical behaviour rivals that of Pt-based catalysts.

Rizzuti *et al.* developed microwave-assisted solvothermal strategies for the controlled synthesis of iron-based composite materials [97,98]. In one study, Fe–Co oxide composites were prepared using ethylene glycol as the solvent and polyvinylpyrrolidone (PVP) as the stabilizer. Microwave irradiation enabled rapid and homogeneous heating, drastically reducing the synthesis time from 12 hours to just 15 minutes compared to conventional methods. Efficient transfer of microwave energy promoted precise control over nucleation and morphology, particularly in the presence of amine additives that directed the formation of well-defined Fe–Co microfibrillar structures. This highlights the tunability and speed of the MW-assisted solvothermal route [97]. Subsequently, the same authors synthesised Fe_3O_4/CeO_2 nanocomposites via a similar microwave-assisted solvothermal method in ethylene glycol. This achieved the rapid and controlled deposition of ceria nanoparticles onto magnetite seeds of various morphologies [98]. Compared to conventional solvothermal procedures, the microwave-assisted approach minimised sintering, enhanced crystallinity and eliminated the need for organic stabilisers. The resulting magnetic nanocomposites displayed excellent catalytic activity in the solvent-free oxidative coupling of benzyl alcohol and aniline to form imines. They were highly recyclable and outperformed commercial CeO_2.

Semeraro et al. reported on the microwave-assisted synthesis of ZnO/γ-Fe_2O_3 nanocomposites for the photodegradation of tetracycline [99]. Microwaves enabled the rapid formation of well-dispersed nanostructures with an increased surface area and porosity. This improved the photocatalytic efficiency by 20%, while also allowing for the catalyst to be recovered magnetically.

González-Rivera and Italian co-workers employed microwave-assisted solvothermal synthesis to fabricate magnetothermally responsive iron oxide–halloysite nanocomposites using a confined phosphorylated nanoreactor [100]. Microwave irradiation, applied via a coaxial antenna inside the solvothermal reactor, enabled rapid and homogeneous thermal activation. This allowed for precise control over the in situ nucleation and growth of superparamagnetic iron oxide nanoparticles. This efficient energy coupling accelerated the urea hydrolysis catalysed by the phosphorylated halloysite lumen and enabled the selective deposition of iron oxide nanoparticles within the inner cavity or on the outer surface of the nanotubes. Compared to conventional heating, the microwave-assisted approach significantly reduced synthesis times, improved structural uniformity and aligned with green chemistry principles. The resulting composites exhibited strong superparamagnetic behaviour and magnetothermal responsiveness, highlighting the effectiveness of microwave-assisted

 doi:10.20944/preprints202511.1382.v1

solvothermal processing in designing multifunctional nanocarriers for use in biomedical and catalytic applications.

Castellino *et al.* [101] developed a N- and S-co-doped rGO/Fe_2O_3 nanocomposite via a fast one-pot microwave-assisted procedure. Iron oxide nanoparticles were incorporated onto the graphene surface without damaging its structure, while sulfur and nitrogen atoms were integrated into the rGO lattice. The synthesis involved dispersing the precursors in deionized water, followed by 30 min of ultrasonication and 15 min of microwave irradiation at 180 °C (800 W). The resulting material exhibited well-dispersed Fe_2O_3 nanocrystals and a co-doped rGO matrix, showing excellent electrochemical performance for oxygen reduction reaction, comparable to commercial Pt/C catalysts.

6. Phosphates, Zeolites, Miscellaneous

Microwave-assisted hydrothermal synthesis has proven to be a highly efficient and versatile method for the preparation of Eu^{3+}-doped YPO_4 (5 mol % Eu) nanophosphors, enabling precise control over particle morphology, size, and optical properties. Paradisi *et al.* reported that well-crystallized, single-phase Eu^{3+}:YPO_4 nanopowders with tetragonal Xenotime-Y structure can be obtained in extremely short times (5–30 minutes) at temperatures between 200 and 240 °C, without the need for post-synthesis calcination. By tuning the microwave reaction parameters, nanocrystals with rice-like or rod-shaped morphologies and narrow size distributions were produced, exhibiting intense red emission upon UV excitation [102]. Further studies have demonstrated the pivotal role of temperature in the crystallisation process, identifying a threshold between 140 and 160 °C for the formation of nanocrystalline material (Figure 7). Higher temperatures promote the coalescence of nanobundles into well-defined nanorods [103].

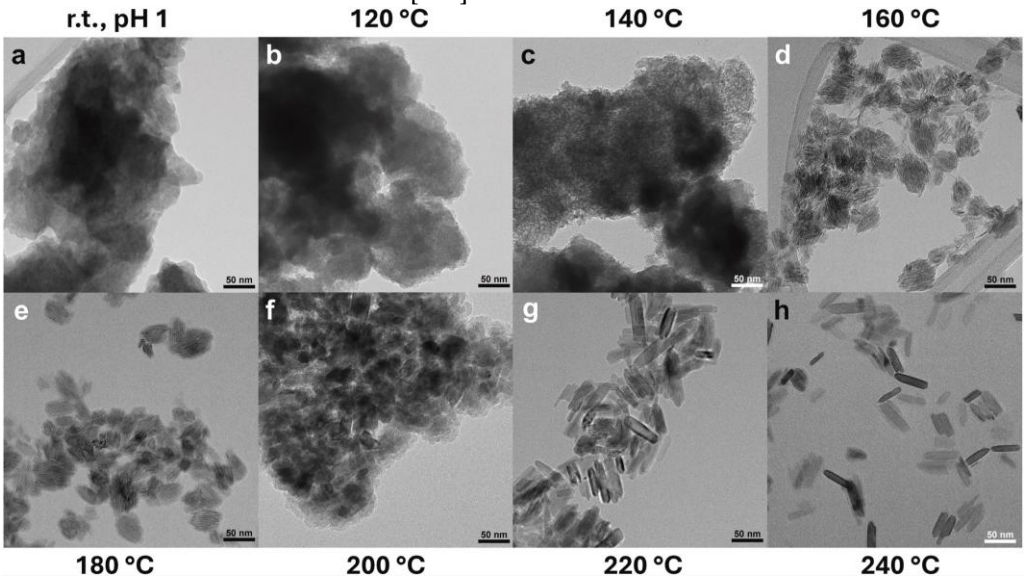

 doi:10.20944/preprints202511.1382.v1

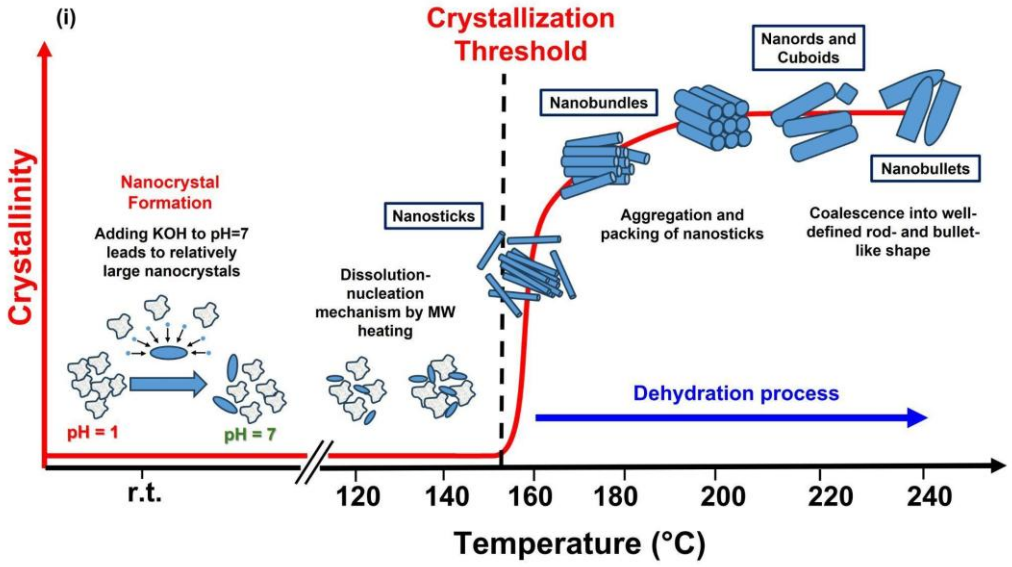

Figure 7. (a-h) TEM micrographs (at 150k magnification) of all Eu^{3+}:YPO_4 samples obtained after precipitation at room temperature at pH = 1 (a) and after 20 min of MW heating at 120 °C (b), 140 °C (c), 160 °C (d), 180 °C (e), 200 °C (f), 220 °C (g) and 240 °C (h). (i) Crystal growth scheme mechanism, adapted from Ref. [103].

Compared with conventional hydrothermal synthesis, which requires prolonged autoclave treatments of at least 12 hours to achieve fully crystalline tetragonal Eu^{3+}:YPO_4, the microwave-assisted method is markedly faster and more energy-efficient. Conventional hydrothermal treatments also lead to time-dependent changes in particle morphology, evolving from nano-needles to rice-like shapes. This affects the surface-to-volume ratio and luminescence efficiency [104]. In contrast, microwave-assisted synthesis enables rapid, homogeneous heating that minimises amorphous residues and allows fine control over particle shape and size. This results in materials with high luminescence efficiency and uniform dopant distribution. These microwave-synthesized nanophosphors have been successfully formulated into water-based luminescent inks for anti-counterfeiting and security printing applications [105].

Furthermore, microwave-assisted techniques have become increasingly important in the synthesis and functionalisation of zeolites, offering several key advantages over conventional methods. These include accelerated crystallisation, greater control over particle size and morphology, greater energy efficiency, and the ability to fine-tune chemical properties such as acidity and ion-exchange capacity. Early studies demonstrated that pure zeolites, such as NaA (sodium aluminosilicate A) and LTA (Linde Type A), could be obtained within one hour under microwave irradiation. The strong dielectric heating effect enabled higher yields and distinct crystal morphologies compared to conventional syntheses [106,107]. Subsequent developments have explored continuous microwave-assisted processes, in which reactor geometry, microwave power and seeding play a critical role in determining crystal size, distribution and overall crystallinity [108]. Microwave heating has also been successfully used to grow zeolite coatings on metallic foams, such as copper and aluminium, for use in heat pumps. For example, SAPO-34 (silicoaluminophosphate with a chabazite framework) and SAPO-44 coatings can be deposited in situ on aluminium foams. Synthesis times are reduced by an order of magnitude compared to conventional hydrothermal methods while adsorption performance is preserved [109,110]. Additionally, microwaves facilitate the hydrothermal conversion of pre-exchanged zeolites into metastable phases such as paracelsian, demonstrating their ability to produce phases that would otherwise be difficult or impossible to obtain under classical conditions [111].

In addition to classical zeolite frameworks, microwave-assisted techniques have also been employed in the production of hybrid micro-mesoporous catalysts. Taghavi and Italian co-workers reported a CuZSM-5@HMS composite, for which microwave-assisted solid-state ion exchange was

 doi:10.20944/preprints202511.1382.v1

employed to incorporate copper into the ZSM-5 (Zeolite Socony Mobil–5) framework [112]. The mesoporous silica HMS (hexagonal mesoporous silica) with a high surface area provided efficient mass transfer pathways for sugars, intermediates, and products during catalytic reactions. Microwave treatment enabled the precise adjustment of the concentration, strength and type of acidic sites in CuZSM-5, while maintaining crystallinity. The resulting CuZ(60%)@HMS composite exhibited optimised Lewis and Brønsted acidity, structural stability under reaction conditions and superior catalytic performance, achieving levulinic acid yields of 45% from glucose and 30% from cellulose. This example demonstrates how microwave-assisted methods can facilitate rapid zeolite crystallisation, tailored acidity and hierarchical porosity, producing catalysts with enhanced activity and selectivity for biomass conversion and other applications.

Microwave-assisted methods have also been successfully employed in the production of hybrid organic-inorganic materials, including organoclays, which combine the ordered, layered structure of clays with functional organic or biological molecules. Villa *et al.* reviewed the use of microwaves at various stages of organoclay synthesis, emphasising the benefits of microwave-assisted hydrothermal techniques for intercalating organic molecules into clay layers. This approach enables rapid, controlled and energy-efficient processing while preserving the structural integrity of the inorganic host and organic molecules. The resulting organoclays exhibit enhanced chemical, catalytic, optical and electronic properties and can be incorporated into polymeric matrices to create advanced hybrid materials [113].

Microwave-assisted techniques can be combined with other innovative activation methods to enhance synthesis efficiency and selectivity further. Martina *et al.* reviewed the combined use of microwaves and ultrasound (or hydrodynamic cavitation) in hybrid technologies, demonstrating its application in both organic and inorganic synthesis. This combined approach enables faster reactions, improved selectivity and significant energy savings while facilitating the design of cleaner, safer processes. Dedicated hybrid reactors have proven particularly effective in preparing nanomaterials and novel green catalysts, providing a versatile platform for process intensification in modern chemistry [114].

7. Metastable Phases

The use of microwave energy as a heating source for combustion synthesis from solid reactants, demonstrated by Dalton *et al.* was focused on the preparation of ceramic materials, mainly carbides, due to excellent MWs absorbing properties of carbon-based reactants [115]. Indeed, due to the well-known inability of bulk metals to efficiently absorb microwave energy—because their high reflectivity and low skin depth prevent effective volumetric heating—the possibility of heating metallic materials was first successfully demonstrated by Roy et al. using metal powders [116]. Some authors have begun exploiting microwave energy to ignite the Self-propagating High-temperature Synthesis (SHS) of Ni and Al powder mixtures to produce a duplex intermetallic coating on Ti substrates as mentioned by Rosa *et al.* in his review [22]. Due to the high exothermic nature of the reaction, the newly formed NiAl is in the liquid phase and can react with the underlying Ti to form a tough ternary intermediate layer, belonging to the Ti–Ni–Al system, in a one step process. Despite the possibility to selectively heat the powders compact, it was also demonstrated that MW heating after the ignition of the exothermic reaction could be used to modify the microstructure of the coating due to a significantly reduction in the cooling rate [117]. The possibility to significantly modify the cooling rates by continuing to transfer microwave energy to the ignited sample was experimentally demonstrated by Rosa et al. for Fe–Al powder compacts by means of both optical pyrometry and a contact sapphire fiber at temperatures of up to 1900°C [118].

Starting from successfully synthesis of pure metal powders as reactants for intermetallics compounds Some of the authors are still working on the preparation of intermetallics [117], functionally graded materials [119], or as a joining technique between dissimilar materials [120]. The advantage of applying microwaves to combustion synthesis reactions resulted in high purity of the

 doi:10.20944/preprints202511.1382.v1

products [121], rapid ignition of the reaction [122], possibility to control the products microstructure [123] and cooling rate after synthesis, especially in presence of ferromagnetic reactants [124].

Since 2017 the Veronesi's research group [125] has been working on synthesis of Heusler alloys [126] and synthesis of HEAs [127] and via powder metallurgy. More efforts have been devoted to the development of HEA synthesis methods, with a particular focus on various mixing routes, including simple blending, mechanical activation for 1 hour, and mechano-synthesis (pre-alloying) via high-energy ball milling [127].

In the meanwhile, authors investigate the effect of adding reactive ceramic particles as reinforcement in HEA to form a metal matrix composite [128]. More recently, the use of microwave-assisted synthesis for producing HEAs from solid scrap generated by metal additive manufacturing has gained attention. This strategy is driven by the increasing emphasis on circular economy models and the pursuit of zero-waste manufacturing practices [129].

Thus exploiting microwave irradiation as a fast heating method to activate combustion synthesis in metal powder offers distinct advantages over conventional methods, such as improved phase purity and reduced synthesis times [130]. The precise control over heating rates and the ability to achieve high temperatures, sometimes exceeding adiabatic combustion temperatures, are crucial for tailoring the microstructure and phase evolution in these systems. The efficiency of microwave heating also contributes to a more uniform temperature distribution throughout the precursor mixture, mitigating issues such as localized overheating or incomplete reactions commonly observed in other synthesis routes. Moreover, the localized energy deposition characteristic of microwave processing can significantly reduce overall energy consumption compared to traditional high-temperature furnaces, which often require extensive heating and cooling cycles for large-scale production [131].

The integration of microwave synthesis with other advanced processing techniques, such as mechanical alloying, can further enhance the stabilization of out-of-equilibrium phases and refine microstructural features, opening new avenues for material design.

8. Conclusions and Perspectives

This article aims to provide an overview of Italian research into the microwave-assisted synthesis of inorganic materials and compounds. While we cannot claim to have collected every single article published over the last 20 years, we believe that we have given visibility to all the research groups that have achieved successful results in this field.

In the first three sections, we have attempted to provide a concise explanation of the material/radiation interactions behind MW-assisted syntheses, and to present the pros and cons of using this uncommon heating source. The specific features of microwave-assisted synthesis might have guided the reader through the article, enabling them to evaluate whether these features have been exploited on a case-by-case basis. For example, the case of combustion synthesis using microwave irradiation to ignite and maintain an exothermic reaction is clear evidence that electromagnetic energy can transfer where heat cannot.

The results published in the literature have been here presented in a way that grouped the different types of compounds together, starting with simple oxides and ending with complex crystalline compounds such as phosphates and zeolites, mentioning last the intermetallic compounds of recent interest.

The applications of compounds produced by microwave-assisted synthesis in either the liquid or solid state were cited for each individual compound, with researchers highlighting the respective advantages and disadvantages of each.

In the perspective of new applications, we expect the special features of dielectric heating to be developed in the search for new, high-performance composite structures and morphologies. This will be achieved by integrating the results obtained over the last 20 years with the capabilities offered by recent developments in solid-state, microwave generator-based reactor technology. With respect to

 doi:10.20944/preprints202511.1382.v1

magnetron, the reduced size and increased controllability of the MW radiation produced using solid state generator, the development of reactors fully dedicated to chemical synthesis may be expected.

We hope that this Review paper generates new interest not only in the pursuit of additional experimental work in inorganic syntheses using microwaves, but also in investigating the mechanisms of microwave-assisted reactions.

Acknowledgments: The authors would like to thank Paolo Veronesi (University of Modena and Reggio Emilia) for his helpful discussions during the preparation of this review. .

Author Contributions: Conceptualization, C.L., E. C., C. M.; writing—original draft preparation, C.L., E. C., C. M.; writing—review and editing, C.L. and C.M.. All authors have read and agreed to the published version of the manuscript.

Conflicts of Interest: The authors declare no conflicts of interest.

References

1. Metaxas, C.; Meredith, R. *Industrial Microwave Heating*; Peter Peregrinus/IEE: Stevenage, UK, 1983; reprinted 1988 and 1993.
2. Thostenson, E.T.; Chou, T.-W. Microwave processing: Fundamentals and applications. *Compos. Part A Appl. Sci. Manuf.* **1999**, *30*, 1055–1071. https://doi.org/10.1016/S1359-835X(99)00020-2.
3. Cravotto, G.; Carnaroglio, D. *Microwave Chemistry*; De Gruyter: Berlin, Germany; Boston, MA, USA, 2017. https://doi.org/10.1515/9783110479935.
4. Fanari, F.; Muntoni, G.; Dachena, C.; Carta, R.; Desogus, F. Microwave Heating Improvement: Permittivity Characterization of Water–Ethanol and Water–NaCl Binary Mixtures. *Energies* **2020**, *13*, 4861. https://doi.org/10.3390/en13184861.
5. Das, A.; Banik, B.K. *Microwaves in Chemistry Applications: Fundamentals, Methods and Future Trends* (Advances in Green and Sustainable Chemistry); Elsevier: Amsterdam, The Netherlands, 2021; ISBN 9780128228951.
6. Zhao, J.; Yan, W. Microwave-assisted Inorganic Syntheses. In *Modern Inorganic Synthetic Chemistry;* Xu, R., Pang, W., Huo, Q., Eds.; Elsevier, The Netherlands, 2011, pp. 173-195. https://doi.org/10.1016/B978-0-444-53599-3.10008-3.
7. Horikoshi, S.; Matsuzaki, S.; Mitani, T.; Serpone, N. Microwave frequency effects on dielectric properties of some common solvents and on microwave-assisted syntheses: 2-Allylphenol and the C12–C2–C12 Gemini surfactant. *Radiat. Phys. Chem.* **2012**, *81*, 1885–1895. https://doi.org/10.1016/j.radphyschem.2012.07.011.
8. Gezahegn, Y.A.; Tang, J.; Sablani, S.S.; Pedrow, P.D.; Hong, Y.-K.; Lin, H.; Tang, Z. Dielectric properties of water relevant to microwave assisted thermal pasteurization and sterilization of packaged foods. *Innov. Food Sci. Emerg. Technol.* **2021**, *74*, 102837. https://doi.org/10.1016/j.ifset.2021.102837.
9. Stuerga, D. Microwave–Material Interactions and Dielectric Properties: Key Ingredients for Mastery of Chemical Microwave Processes. In *Microwaves in Organic Synthesis*; Loupy, A., Ed.; Wiley-VCH: Weinheim, Germany, 2006. https://doi.org/10.1002/9783527619559.ch1.
10. Tang, J. Unlocking Potentials of Microwaves for Food Safety and Quality. *J. Food Sci.* **2015**, *80*, E1776–E1793. https://doi.org/10.1111/1750-3841.12959.
11. Peng, J.; Tang, J.; Jiao, Y.; Bohnet, S.G.; Barrett, D.M. Dielectric Properties of Tomatoes Assisting in the Development of Microwave Pasteurization and Sterilization Processes. *LWT—Food Sci. Technol.* **2013**, *54*, 367–376. https://doi.org/10.1016/j.lwt.2013.07.006.
12. Binner, J.; Al-Dawery, I.; Aneziris, C.; et al. Use of the Inverse Temperature Profile in Microwave Processing of Advanced Ceramics. *MRS Online Proc. Libr.* **1992**, *269*, 357–362. https://doi.org/10.1557/PROC-269-357.
13. Priecel, P.; Lopez-Sanchez, J.A. Advantages and Limitations of Microwave Reactors: From Chemical Synthesis to the Catalytic Valorization of Biobased Chemicals. *ACS Sustain. Chem. Eng.* **2019**, *7*, 3–21. https://doi.org/10.1021/acssuschemeng.8b03286.

14. Bogdał, D.; Prociak, A. *Microwave-Enhanced Polymer Chemistry and Technology*; Wiley-Blackwell: Ames, IA, USA, 2007. https://doi.org/10.1002/9780470390276..
15. Kappe, C.O.; Stadler, A.; Dallinger, D. *Microwaves in Organic and Medicinal Chemistry*; Wiley-VCH: Weinheim, Germany, 2012. https://doi.org/10.1002/3527606556.
16. Singh, J.; Lathwal, A.; Agarwal, S.; Nath, M. Microwave-Accelerated Approaches to Diverse Xanthenes: A Review. *Curr. Microw. Chem.* **2020**, *7*, 99–111. https://doi.org/10.2174/221333560799920041.
17. Gulati, S.; John, S.E.; Shankaraiah, N. Microwave-Assisted Multicomponent Reactions in Heterocyclic Chemistry and Mechanistic Aspects. *Beilstein J. Org. Chem.* **2021**, *17*, 819–865. https://doi.org/10.3762/bjoc.17.71.
18. Jacob, J.; Chia, L.H.L.; Boey, F.Y.C. Thermal and Nonthermal Interaction of Microwave Radiation with Materials. *J. Mater. Sci.* **1995**, *30*, 5321–5327.
19. de la Hoz, A.; Díaz-Ortiz, A.; Moreno, A. Review on Non-Thermal Effects of Microwave Irradiation in Organic Synthesis. *J. Microw. Power Electromagn. Energy* **2006**, *41*, 45–66.
20. de la Hoz, A.; Díaz-Ortiz, A.; Moreno, A. Microwaves in Organic Synthesis: Thermal and Non-Thermal Microwave Effects. *Chem. Soc. Rev.* **2005**, *34*, 164–178.
21. Perreux, L.; Loupy, A.; Petit, A. Nonthermal Effects of Microwaves in Organic Synthesis. In *Microwaves in Organic Synthesis*; de la Hoz, A., Loupy, A., Eds.; Wiley-VCH: Weinheim, Germany, 2013. https://doi.org/10.1002/9783527651313.ch.
22. Rosa, R.; Trombi, L.; Veronesi, P.; et al. Microwave Energy Application to Combustion Synthesis: A Comprehensive Review of Recent Advancements and Most Promising Perspectives. *Int. J. Self-Propag. High-Temp. Synth.* **2017**, *26*, 221–233. https://doi.org/10.3103/S1061386217040057.
23. Komarneni, S.; Roy, R. Titania Gel Spheres by a New Sol–Gel Process. *Mater. Lett.* **1985**, *3*, 165–167.
24. Komarneni, S. Microwave Memories. *Chem. World* **2009**, *6*, 38.
25. Leonelli, C.; Komarneni, S. Inorganic Syntheses Assisted by Microwave Heating. *Inorganics* **2015**, *3(4)*, 388–391. https://doi.org/10.3390/inorganics3040388.
26. Komarneni, S.; Roy, R.; Li, Q.H. Microwave-Hydrothermal Synthesis of Ceramic Powders. *Mater. Res. Bull.* 1992, *27*, 1393–1405.
27. Walkiewicz, J.W.; Kazonich, G.; McGill, S.L. Microwave heating characteristics of selected minerals and compounds. *Miner. Metall. Process.* **1988**, *5*, 39.
28. Rawat, S.; Samyal, R.; Bedi, R.; Bagha, A.K. Comparative Performance of Various Susceptor Materials and Vertical Cavity Shapes for Selective Microwave Hybrid Heating (SMHH). *Phys. Scr.* **2022**, *97*, 125704. https://doi.org/10.1088/1402-4896/ac9e7d.
29. Martina, K.; Cravotto, G.; Varma, R.S. Impact of Microwaves on Organic Synthesis and Strategies toward Flow Processes and Scaling Up. *J. Org. Chem.* **2021**, *86*, 13857–13872. https://doi.org/10.1021/acs.joc.1c00865.
30. Pal, M.; Sehgal, S.; Kumar, H. Optimization of Elemental Weight % in Microwave-Processed Joints of SS304/SS316 Using Taguchi Philosophy. *J. Adv. Manuf. Syst.* **2020**, *19*, 543–565. https://doi.org/10.1142/S0219686720500262.
31. Rao, K.J.; Vaidhyanathan, B.; Ganguli, M.; Ramakrishnan, P.A. Synthesis of Inorganic Solids Using Microwaves. *Chem. Mater.* **1999**, *11*, 882–895.
32. Leonelli, C.; Łojkowski, W. Main Development Directions in the Application of Microwave Irradiation to the Synthesis of Nanopowders. *Chem. Today* **2007**, *25*, 34–38.
33. Leonelli, C.; Łojkowski, W.; Veronesi, P. Temperature Profile within a Microwave-Irradiated Batch Reactor. *J. Mach. Constr. Maint.* **2018**, *3*, 33–40.
34. Łojkowski, W.; Gedanken, A.; Grzanka, E.; et al. Solvothermal Synthesis of Nanocrystalline Zinc Oxide Doped with Mn^{2+}, Ni^{2+}, Co^{2+} and Cr^{3+} Ions. *J. Nanopart. Res.* **2009**, *11*, 1991–2002. https://doi.org/10.1007/s11051-008-9559-9.
35. Nicollet, C.; Carrillo, A.J. Back to Basics: Synthesis of Metal Oxides. *J. Electroceram.* **2024**, *52*, 10–28. https://doi.org/10.1007/s10832-023-00340-y.
36. Rosa, R.; Ponzoni, C.; Leonelli, C. Direct Energy Supply to the Reaction Mixture during Microwave-Assisted Hydrothermal and Combustion Synthesis of Inorganic Materials. *Inorganics* **2014**, *2*, 191-210. https://doi.org/10.3390/inorganics2020191.

37. Trocino, S.; Prakash, T.; Jayaprakash, J.; Donato, A.; Neri, G.; Donato, N. Electrical Characterization of Nanostructured Sn-Doped ZnO Gas Sensors. In *Sensors*; Compagnone, D., Baldini, F., Di Natale, C., Betta, G., Siciliano, P., Eds.; Lecture Notes in Electrical Engineering; Springer: Cham, Switzerland, 2015; Volume 319. https://doi.org/10.1007/978-3-319-09617-9_34.
38. Prakash, T.; Neri, G.; Bonavita, A.; Ranjith Kumar, E.; Gnanamoorthi, K. Structural, Morphological and Optical Properties of Bi-Doped ZnO Nanoparticles Synthesized by a Microwave Irradiation Method. *J. Mater. Sci. Mater. Electron.* **2015**, *26*, 4913–4921. https://doi.org/10.1007/s10854-015-3002-7.
39. Gionco C.; Fabbri D.; Calza P.; Paganini M.C. Synthesis, Characterization, and Photocatalytic Tests of N-Doped Zinc Oxide: A New Interesting Photocatalyst. *J. Nanomaterials* **2016**, *2016*, 4129864. https://doi.org/10.1155/2016/4129864.
40. Garino, N.; Limongi, T.; Dumontel, B.; Canta, M.; Racca, L.; Laurenti, M.; Castellino, M.; Casu, A.; Falqui, A.; Cauda, V. A Microwave-Assisted Synthesis of Zinc Oxide Nanocrystals Finely Tuned for Biological Applications. Nanomaterials 2019, 9, 212. https://doi.org/10.3390/nano9020212.
41. Garino, N.; Sanvitale, P.; Dumontel, B.; Laurenti, M.; Colilla, M.; Izquierdo-Barba, I.; Cauda, V.; Vallet-Regí, M. Zinc Oxide Nanocrystals as a Nanoantibiotic and Osteoinductive Agent. *RSC Adv.* **2019,** *9*, 11312–11321. https://doi.org/10.1039/C8RA10236H.
42. Gautier di Confiengo, G.; Faga, M.G.; La Parola, V.; Magnacca, G.; Paganini, M.C.; Testa, M.L. Microwave Approach and Thermal Decomposition: A Sustainable Way to Produce ZnO Nanoparticles with Different Chemo-Physical Properties. *Mater. Chem. Phys.* 2024, *321*, 129485. https://doi.org/10.1016/j.matchemphys.2024.129485.
43. Natile, M.M., Boccaletti, G., Glisenti, A., Properties and reactivity of nanostructured CeO2 powders: Comparison among two synthesis procedures, *Chem. Matls* **2005**, *17(25),* 6272–6286, https://doi.org/10.1021/cm051352d.
44. Natile M.M., Glisenti A. Nanostructured CeO_2 powders by XPS, *Surf. Sci. Spectra* **2006**, *13(1-4),* 17-30. https://doi.org/10.1116/11.20060401.
45. Bonamartini Corradi, A.; Bondioli, F.; Ferrari, A.M.; Manfredini, T. Synthesis and Characterization of Nanosized Ceria Powders by Microwave–Hydrothermal Method. *Mater. Res. Bull.* **2006**, *41*, 38–44. https://doi.org/10.1016/j.materresbull.2005.07.044.
46. Gondolini, A.; Mercadelli, E.; Sanson, A.; Albonetti, S.; Doubova, L.; Boldrini, S. Microwave-Assisted Synthesis of Gadolinia-Doped Ceria Powders for Solid Oxide Fuel Cells. *Ceram. Int.* **2011**, *37*, 1423–1426. https://doi.org/10.1016/j.ceramint.2011.01.010.
47. Mercadelli, E.; Ghetti, G.; Sanson, A.; Bonelli, R.; Albonetti, S. Synthesis of CeO_2 Nano-Aggregates of Complex Morphology. *Ceram. Int.* **2013**, *39*, 629–634. https://doi.org/10.1016/j.ceramint.2012.06.074.
48. Salusso, D.; Grillo, G.; Manzoli, M.; Signorile, M.; Zafeiratos, S.; Barreau, M.; Damin, A.; Crocellà, V.; Cravotto, G.; Bordiga, S. CeO_2 Frustrated Lewis Pairs Improving CO_2 and CH_3OH Conversion to Monomethylcarbonate. *ACS Appl. Mater. Interfaces* **2023**, *15*, 15396–15408. https://doi.org/10.1021/acsami.2c22122.
49. Ballauri, S.; Sartoretti, E.; Castellino, M.; Armandi, M.; Piumetti, M.; Fino, D.; Russo, N.; Bensaid, S. Mesoporous Ceria and Ceria–Praseodymia as High Surface Area Supports for Pd-Based Catalysts with Enhanced Methane Oxidation Activity. *ChemCatChem* **2024**, *16*, e202301359. https://doi.org/10.1002/cctc.202301359.
50. Conciauro, F.; Filippo, E.; Carlucci, C.; Vergaro, V.; Baldassarre, F.; D'Amato, R.; Terranova, G.; Lorusso, C.; Congedo, P.M.; Scremin, B.F.; Ciccarella, G. Properties of Nanocrystals-Formulated Aluminosilicate Bricks. *Nanomaterials Nanotechnol*. **2015**, *5*, 28. https://doi.org/10.5772/61068.
51. Zhang, R.; Santangelo, S.; Fazio, E.; Neri, F.; D'Arienzo, M.; Morazzoni, F.; Zhang, Y.; Pinna, N.; Russo, P.A. Stabilization of Titanium Dioxide Nanoparticles at the Surface of Carbon Nanomaterials Promoted by Microwave Heating. *Chem.—Eur. J.* **2015**, *21*, 14901–14910. https://doi.org/10.1002/chem.201502433.
52. Filippo, E.; Carlucci, C.; Capodilupo, A. L.; Perulli, P.; Conciauro, F.; Corrente, G. A.; Gigli, G.; Ciccarella, G. Enhanced Photocatalytic Activity of Pure Anatase TiO_2 and Pt–TiO_2 Nanoparticles Synthesized by Green Microwave Assisted Route. *Mater. Res.* **2015**, *18*, 473–481. https://doi.org/10.1590/1516-1439.301914.

 doi:10.20944/preprints202511.1382.v1

53. Filippo, E.; Carlucci, C.; Capodilupo, P.; Perulli, P.; Conciauro, F.; Corrente, G. A.; Gigli, G.; Ciccarella, G. Facile Preparation of TiO_2–Polyvinyl Alcohol Hybrid Nanoparticles with Improved Visible Light Photocatalytic Activity. *Appl. Surf. Sci.* **2015**, *331*, 292–298. https://doi.org/10.1016/j.apsusc.2014.12.112.
54. Tian, F.; Wu, Z.; Tong, Y.; Cravotto, G. Microwave-Assisted Synthesis of Carbon-Based (N, Fe)-Codoped TiO_2 for the Photocatalytic Degradation of Formaldehyde. *Nanoscale Res. Lett.* **2015**, *10*, 360. https://doi.org/10.1186/s11671-015-1061-6.
55. Kőrösi, L.; Bognár, B.; Bouderias, S.; Castelli, A.; Scarpellini, A.; Pasquale, L.; Prato, M. Highly-Efficient Photocatalytic Generation of Superoxide Radicals by Phase-Pure Rutile TiO_2 Nanoparticles for Azo Dye Removal. *Appl. Surf. Sci.* **2019**, *493*, 719–728. https://doi.org/10.1016/j.apsusc.2019.06.259.
56. Alfano, B.; Miglietta, M. L.; Polichetti, T.; Massera, E.; Veneri, P. D. Titanium Dioxide Doped Graphene for Ethanol Detection at Room Temperature. In *Sensors and Microsystems*. AISEM 2020; Di Francia, G., Di Natale, C., Eds.; Lecture Notes in Electrical Engineering, Vol. 753; Springer: Cham, 2021; pp 169–177. https://doi.org/10.1007/978-3-030-69551-4_15.
57. Paradisi, E.; Rosa, R.; Baldi, G.; Dami, V.; Cioni, A.; Lorenzi, G.; Leonelli, C. Effect of isopropanol co-product on the long-term stability of TiO_2 nanoparticle suspensions produced by microwave-assisted synthesis. *Chem. Eng. Process. – Process Intensif.* **2021**, *159*, 108242. https://doi.org/10.1016/j.cep.2020.108242.
58. Paradisi, E.; Rosa, R.; Baldi, G.; Dami, V.; Cioni, A.; Lorenzi, G.; Leonelli, C. Microwave-Assisted Vacuum Synthesis of TiO_2 Nanocrystalline Powders in One-Pot, One-Step Procedure. *Nanomaterials* **2022**, *12*, 149. https://doi.org/10.3390/nano12010149.
59. Paradisi, E.; Mortalò, C.; Russo, P.; Zin, V.; Miorin, E.; Montagner, F.; Leonelli, C.; Deambrosis, S.M. Facile and Effective Method for the Preparation of Sodium Alginate/TiO_2 Bio-Composite Films for Different Applications. *Macromol. Symp*. **2024**, *413*, 2300230. https://doi.org/10.1002/masy.202300230.
60. Paradisi, E.; Plaza-González, P. J.; Baldi, G.; Catalá-Civera, J. M.; Leonelli, C. On the use of microwaves during combustion/calcination of N-doped TiO_2 precursor: An EMW absorption study combined with TGA-DSC-FTIR results. *Mater. Lett.* **2023**, *338*, 133975. https://doi.org/10.1016/j.matlet.2023.133975.
61. Paradisi, E.; Lassinantti Gualtieri, M.; Veronesi, P.; Dami, V.; Lorenzi, G.; Cioni, A.; Baldi, G.; Leonelli, C. Crucible Effect on Phase Transition Temperature during Microwave Calcination of a N-Doped TiO_2 Precursor: Implications for the Preparation of TiO_2 Nanophotocatalysts. *ACS Appl. Nano Mater*. **2023**, *6*, 5448–5459. https://doi.org/10.1021/acsanm.3c00584.
62. Carlucci, C.; Scremin, B.F.; Sibillano, T.; Giannini, C.; Filippo, E.; Perulli, P.; Capodilupo, A.L.; Corrente, G.A.; Ciccarella, G. Microwave-assisted synthesis of boron-modified TiO_2 nanocrystals. *Inorganics* **2014**, *2*, 264–277.
63. Spepi, A.; Duce, C.; Ferrari, C.; González-Rivera, J.; Jagličić, Z.; Domenici, V.; Pineider, F.; Tiné, M. R. A simple and versatile solvothermal configuration to synthesize superparamagnetic iron oxide nanoparticles using a coaxial microwave antenna. *RSC Adv.* **2016**, 6, 104366. https://doi.org/10.1039/C6RA17513A.
64. Muhyuddin, M.; Testa, D.; Lorenzi, R.; Vanacore, G. M.; Poli, F.; Soavi, F.; Specchia, S.; Giurlani, W.; Innocenti, M.; Rosi, L.; Santoro, C. Iron-based electrocatalysts derived from scrap tires for oxygen reduction reaction: Evolution of synthesis-structure-performance relationship in acidic, neutral and alkaline media. *Electrochim. Acta* **2022**, *433*, 141254. https://doi.org/10.1016/j.electacta.2022.141254.
65. Porru, M.; Morales, M.d.P.; Gallo-Cordova, A.; Espinosa, A.; Moros, M.; Brero, F.; Mariani, M.; Lascialfari, A.; Ovejero, J.G. Tailoring the Magnetic and Structural Properties of Manganese/Zinc Doped Iron Oxide Nanoparticles through Microwaves-Assisted Polyol Synthesis. *Nanomaterials* **2022**, *12*, 3304. https://doi.org/10.3390/nano12193304.
66. Saladino, G.M.; Hamawandi, B.; Vogt, C.; Gunaratna, K.; Rajarao, R.; Toprak, M.S. Click Chemical Assembly and Validation of Bio-Functionalized Superparamagnetic Hybrid Microspheres. *Appl. Nanosci.* **2020**, *10*, 1861–1869. https://doi.org/10.1007/s13204-020-01274-5.
67. Saladino, G.M.; Hamawandi, B.; Demir, M.A.; Yazgan, I.; Toprak, M.S. A Versatile Strategy to Synthesize Sugar Ligand Coated Superparamagnetic Iron Oxide Nanoparticles and Investigation of Their Antibacterial Activity. *Colloids Surf. A Physicochem. Eng. Asp.* **2021**, *613*, 126086. https://doi.org/10.1016/j.colsurfa.2020.126086.

68. Saladino, G.M.; Kakadiya, R.; Ansari, S.R.; Teleki, A.; Toprak, M.S. Magnetoresponsive Fluorescent Core–Shell Nanoclusters for Biomedical Applications. *Nanoscale Adv*. **2023**, *5*, 1323. https://doi.org/10.1039/d2na00887d.
69. Mekseriwattana, W.; Silvestri, N.; Brescia, R.; Tiryaki, E.; Barman, J.; Mohammadzadeh, F.G.; Jarmouni, N.; Pellegrino, T. Shape-Control in Microwave-Assisted Synthesis: A Fast Route to Size-Tunable Iron Oxide Nanocubes with Benchmark Magnetic Heat Losses. *Adv. Funct. Mater.* **2025**, *35*, 2413514. https://doi.org/10.1002/adfm.202413514.
70. Calsolaro, F.; Garello, F.; Cavallari, E.; Magnacca, G.; Trukhan, M.V.; Valsania, M.C.; Cravotto, G.; Terreno, E.; Martina, K. Amphoteric β-Cyclodextrin Coated Iron Oxide Magnetic Nanoparticles: New Insights into Synthesis and Application in MRI. *Nanoscale Adv.* **2025**, *7*, 155. https://doi.org/10.1039/D4NA00692E.
71. Bondioli, F.; Ferrari, A. M.; Leonelli, C.; Siligardi, C.; Pellacani, G. C. Microwave-hydrothermal synthesis of nanocrystalline zirconia powders. *J. Am. Ceram. Soc.* **2001**, *84*, 2728–2730. https://doi.org/10.1111/j.1151-2916.2001.tb01084.x.
72. Bondioli, F.; Ferrari, A. M.; Braccini, S.; Leonelli, C.; Pellacani, G. C.; Opalińska, A.; Chudoba, T.; Grzanka, E.; Palosz, B. F.; Łojkowski, W. Microwave–hydrothermal synthesis of nanocrystalline Pr-doped zirconia powders at pressures up to 8 MPa. *Solid State Phenom.* **2003**, *94*, 193–196. https://doi.org/10.4028/www.scientific.net/ssp.94.193.
73. Bondioli, F.; Leonelli, C.; Manfredini, T.; Ferrari, A. M.; Caracoche, M. C.; Rivas, P. C.; Rodríguez, A. M. Microwave-hydrothermal synthesis and hyperfine characterization of praseodymium-doped nanometric zirconia powders. *J. Am. Ceram. Soc.* **2005**, *88*, 633–638. https://doi.org/10.1111/j.1551-2916.2005.00093.x.
74. Rizzuti, A.; Leonelli, C.; Corradi, A.; Caponetti, E.; Martino, D.C.; Nasillo, G.; Saladino, M.L. Structural Characterization of Zirconia Nanoparticles Prepared by Microwave-Hydrothermal Synthesis. *J. Dispersion Sci. Technol.* **2009**, *30*, 1511–1516. https://doi.org/10.1080/01932690903123676.
75. Rizzuti, A.; Corradi, A.; Leonelli, C.; Rosa, R.; Pielaszek, R.; Łojkowski, W. Microwave Technique Applied to the Hydrothermal Synthesis and Sintering of Calcia Stabilized Zirconia Nanoparticles. *J. Nanopart. Res.* **2010**, *12*, 327–335. https://doi.org/10.1007/s11051-009-9619-9.
76. Riva, V.; Boccaccini, D.; Cannio, M.; Maioli, M.; Valle, M.; Romagnoli, M.; Mortalò, C.; Leonelli, C. Insight into t→m Transition of MW Treated 3Y-PSZ Ceramics by Grazing Incidence X-Ray Diffraction. *J. Eur. Ceram. Soc.* **2022**, *42*, 227–237. https://doi.org/10.1016/j.jeurceramsoc.2021.09.054.
77. Giordana, A.; Pizzolitto, C.; Ghedini, E.; Signoretto, M.; Operti, L.; Cerrato, G. Innovative Synthetic Approaches for Sulphate-Promoted Catalysts for Biomass Valorisation. *Catalysts* **2023**, *13*, 1094. https://doi.org/10.3390/catal13071094.
78. Corradi, A.B.; Bondioli, F.; Ferrari, A.M.; Focher, B.; Leonelli, C. *Powder Technol*. **2006**, *167*, 45–48. https://doi.org/10.1016/j.powtec.2006.05.009.
79. Krishnakumar, T.; Pinna, N.; Bonavita, A.; Micali, G.; Rizzo, G.; Neri, G. Microwave-Assisted Synthesis of Metal Oxide Nanostructures for Sensing Applications In *Sensors and Microsystems*; Neri, G., Donato, N., d'Amico, A., Di Natale, C., Eds.; Lecture Notes in Electrical Engineering; Springer: Dordrecht, The Netherlands, 2011; Vol. 91, pp. 55–59. https://doi.org/10.1007/978-94-007-1324-6_7.
80. Sathya Raj, D.; Krishnakumar, T.; Jayaprakash, R.; Prakash, T.; Leonardi, G.; Neri, G. CO Sensing Characteristics of Hexagonal-Shaped CdO Nanostructures Prepared by Microwave Irradiation. *Sensors Actuators B Chem*. **2012**, *171–172*, 853–859. https://doi.org/10.1016/j.snb.2012.05.083.
81. Rajesh, N.; Kannan, J.C.; Krishnakumar, T.; Leonardi, S.G.; Neri, G. Sensing Behavior to Ethanol of Tin Oxide Nanoparticles Prepared by Microwave Synthesis with Different Irradiation Time. *Sensors Actuators B Chem*. **2014**, *194*, 96–104. https://doi.org/10.1016/j.snb.2013.12.060.
82. Bondioli, F.; Corradi, A. B.; Ferrari, A. M.; Leonelli, C.; Siligardi, C.; Manfredini, T.; Evans, N. G. Microwave synthesis of Al_2O_3/Cr_2O_3 (SS) ceramic pigments. J. *Microw. Power Electromagn. Energy* **1998**, *33(1)*, 18–23. https://doi.org/10.1080/08327823.1998.11688354.
83. Bonometti, E.; Castiglioni, M.; Lausarot, P. Solid-state mixed oxides synthesis under microwave heating (JMSL10627-04). *J. Mater. Sci.* **2006**, *41*, 6485–6487. https://doi.org/10.1007/s10853-006-0726-z.
84. Arbizzani, C.; Beninati, S.; Damen, L.; Mastragostino, M. Power and temperature controlled microwave synthesis of SVO. *Solid State Ionics* **2007**, *178(5–6)*, 393–398. https://doi.org/10.1016/j.ssi.2007.01.022.

 doi:10.20944/preprints202511.1382.v1

85. Barison, S.; Fabrizio, M.; Fasolin, S.; Montagner, F.; Mortalò, C. A microwave-assisted sol–gel Pechini method for the synthesis of $BaCe_{0.65}Zr_{0.20}Y_{0.15}O_{3-\delta}$ powders. *Mater. Res. Bull.* **2010**, *45*, 1171–1176. https://doi.org/10.1016/j.materresbull.2010.05.021.
86. Boldrini, S.; Mortalò, C.; Fasolin, S.; Agresti, F.; Doubova, L.; Fabrizio, M.; Barison, S. Influence of microwave-assisted Pechini method on $La_{0.80}Sr_{0.20}Ga_{0.83}Mg_{0.17}O_{3-\delta}$ ionic conductivity. *Fuel Cells* **2012**, *12*, 54–60. https://doi.org/10.1002/fuce.201100058.
87. Ponzoni, C.; Rosa, R.; Cannio, M.; Buscaglia, V.; Finocchio, E.; Nanni, P.; Leonelli, C. Optimization of BFO microwave-hydrothermal synthesis: Influence of process parameters. *J. Alloys Compd.* **2013**, *558*, 150–159. https://doi.org/10.1016/j.jallcom.2013.01.039.
88. Ponzoni, C.; Cannio, M.; Boccaccini, D. N.; Bahl, C. R. H.; Agersted, K.; Leonelli, C. Ultrafast microwave hydrothermal synthesis and characterization of Bi_1−xLaxFeO$_3$ micronized particles. *Mater. Chem. Phys.* **2015**, *162*, 69–75. https://doi.org/10.1016/j.matchemphys.2015.05.002.
89. Ruffo, A.; Mozzati, M.C.; Albini, B.; Galinetto, P.; Bini, M. Role of non-magnetic dopants (Ca, Mg) in $GdFeO_3$ perovskite nanoparticles obtained by different synthetic methods: structural, morphological and magnetic properties. *J. Mater. Sci.: Mater. Electron.* **2020**, *31*, 18263–18277. https://doi.org/10.1007/s10854-020-04374-8.
90. Wu, Z.; Xue, Y.; He, X.; Li, Y.; Yang, X.; Wu, Z.; Cravotto, G. Surfactants-assisted preparation of $BiVO_4$ with novel morphologies via microwave method and CdS decoration for enhanced photocatalytic properties. *J. Hazard. Mater.* **2020**, *387*, 122019. https://doi.org/10.1016/j.jhazmat.2020.122019.
91. Mortalò, C.; Rosa, R.; Veronesi, P.; Fasolin, S.; Zin, V.; Deambrosis, S.M.; Miorin, E.; Dimitrakis, G.; Fabrizio, M.; Leonelli, C. Microwave Assisted Sintering of Na-β''-Al_2O_3 in Single Mode Cavities: Insights in the Use of 2450 MHz Frequency and Preliminary Experiments at 5800 MHz. *Ceram. Int.* **2020**, *46*, 28767–28777. https://doi.org/10.1016/j.ceramint.2020.08.039.
92. Dell'Agli, G.; Mascolo, M. C.; Mascolo, G. Hydrothermal Synthesis of Precursors for Y-TZP/α-Al_2O_3 Composite. *Powder Technol.* **2004**, *148*, 7–10. https://doi.org/10.1016/j.powtec.2004.09.012.
93. Barison, S.; Fabrizio, M.; Mortalò, C.; Antonucci, P. L.; Modafferi, V.; Gerbasi, R. Novel Ru/$La_{0.75}Sr_{0.25}Cr_{0.5}Mn_{0.5}O_{3-\delta}$ catalysts for propane reforming in IT-SOFCs. *Solid State Ionics* **2010**, *181* (5–7), 285–291. https://doi.org/10.1016/j.ssi.2010.01.002.
94. Neri, G.; Leonardi, S.G.; Latino, M.; Donato, N.; Baek, S.; Conte, D.E.; Russo, P.A.; Pinna, N. Sensing Behavior of SnO_2/Reduced Graphene Oxide Nanocomposites toward NO_2. *Sensors Actuators B Chem.* **2013**, *179*, 61–68. https://doi.org/10.1016/j.snb.2012.10.031.
95. Tian, F.; Wu, Z.; Chen, Q.; Yan, Y.; Cravotto, G.; Wu, Z. Microwave-Induced Crystallization of AC/TiO_2 for Improving the Performance of Rhodamine B Dye Degradation. *Appl. Surf. Sci.* **2015**, *351*, 104–112. https://doi.org/10.1016/j.apsusc.2015.05.133.
96. Garino, N.; Sacco, A.; Castellino, M.; Muñoz-Tabares, J. A.; Armandi, M.; Chiodoni, A.; Pirri, C. F. One-pot microwave-assisted synthesis of reduced graphene oxide/iron oxide nanocomposite catalyst for the oxygen reduction reaction. *Chemistry Select* **2016**, *1*, 3640–3648. https://doi.org/10.1002/slct.201601037.
97. Rizzuti, A.; Leonelli, C.; Dell'Anna, M. M.; Romanazzi, G.; Mali, M.; Catauro, M.; Mastrorilli, P. Microwave-assisted solvothermal controlled synthesis of Fe–Co composite material. *Macromol. Symp.* **2021**, *395*, 2000196. https://doi.org/10.1002/masy.202000196.
98. Rizzuti, A.; Dipalo, M. C.; Allegretta, I.; Terzano, R.; Cioffi, N.; Mastrorilli, P.; Mali, M.; Romanazzi, G.; Nacci, A.; Dell'Anna, M. M. Microwave-assisted solvothermal synthesis of Fe_3O_4/CeO_2 nanocomposites and their catalytic activity in the imine formation from benzyl alcohol and aniline. *Catalysts* **2020**, *10*, 1325. https://doi.org/10.3390/catal10111325.
99. Semeraro, P.; Bettini, S.; Sawalha, S.; Pal, S.; Licciulli, A.; Marzo, F.; Lovergine, N.; Valli, L.; Giancane, G. Photocatalytic Degradation of Tetracycline by ZnO/γ-Fe_2O_3 Paramagnetic Nanocomposite Material. *Nanomaterials* **2020**, *10*, 1458. https://doi.org/10.3390/nano10081458.
100. González-Rivera, J.; Spepi, A.; Ferrari, C.; Tovar-Rodriguez, J.; Fantechi, E.; Pineider, F.; Vera-Ramírez, M. A.; Tiné, M. R.; Duce, C. Magnetothermally-responsive nanocarriers using confined phosphorylated halloysite nanoreactor for in situ iron oxide nanoparticle synthesis: A MW-assisted solvothermal approach. *Colloids Surf. A Physicochem. Eng. Asp.* **2022**, *635*, 128116. https://doi.org/10.1016/j.colsurfa.2021.128116.

 doi:10.20944/preprints202511.1382.v1

101. Castellino, M.; Sacco, A.; Fontana, M.; Chiodoni, A.; Pirri, C.F.; Garino, N. The Effect of Sulfur and Nitrogen Doping on the Oxygen Reduction Performance of Graphene/Iron Oxide Electrocatalysts Prepared by Using Microwave-Assisted Synthesis. *Nanomaterials* **2024**, *14*, 560. https://doi.org/10.3390/nano14070560.
102. Paradisi, E.; Mortalò, C.; Zin, V.; Armetta, F.; Boiko, V.; Hreniak, D.; Zapparoli, M.; Deambrosis, S.M.; Miorin, E.; Leonelli, C.; Saladino, M.L. Eu-Doped YPO_4 Luminescent Nanopowders for Anticounterfeiting Applications: Tuning Morphology and Optical Properties by a Rapid Microwave-Assisted Hydrothermal Method. *ACS Appl. Nano Mater*. **2024**, *7*, 6893–6905. https://doi.org/10.1021/acsanm.3c05806.
103. Paradisi, E.; Mortalò, C.; Zin, V.; Deambrosis, S.M.; Zapparoli, M.; Miorin, E.; Leonelli, C. Understanding the Effect of Temperature on the Crystallization of Eu^{3+}:YPO_4 Nanophosphors Prepared by MW-Assisted Method. *Ceram. Int.* **2025**, *51*, 7075–7086. https://doi.org/10.1016/j.ceramint.2024.12.144.
104. Armetta, F.; Boiko, V.; Hreniak, D.; Mortalò, C.; Leonelli, C.; Barbata, L.; Saladino, M.L. Effect of Hydrothermal Time on the Forming Specific Morphology of YPO_4:Eu^{3+} Nanoparticles for Dedicated Luminescent Applications as Optical Markers. *Ceram. Int.* **2023**, *49*, 23287–23294. https://doi.org/10.1016/j.ceramint.2023.04.159.
105. Paradisi, E.; Mortalò, C.; Andreola, F.; Zin, V.; Capelli, R.; Pasquali, L.; Deambrosis, S.M.; Miorin, E.; Leonelli, C. Stable Water-Based Luminescent Suspensions of Eu^{3+}:YPO_4 Nanophosphors in Sodium Alginate Medium: Sustainable Inks for Potential Anticounterfeiting Applications. *Ceram. Int*. **2025**, *51*, 58745-58755. https://doi.org/10.1016/j.ceramint.2025.10.092.
106. Bonaccorsi, L.; Proverbio, E. Microwave assisted crystallization of zeolite A from dense gels. *J. Cryst. Growth* **2003**, *247*, 555–562. https://doi.org/10.1016/S0022-0248(02)02053-5.
107. Bonaccorsi, L.; Proverbio, E. Hydrothermal Synthesis of Zeolite LTA by Microwave Irradiation. *Mater. Res. Innov*. **2004**, *8*, 53–57. https://doi.org/10.1080/14328917.2004.11784828.
108. Bonaccorsi, L.; Proverbio, E. Influence of process parameters in microwave continuous synthesis of zeolite LTA. *Micropor. Mesopor. Mater.* **2008**, *112*, 481–493. https://doi.org/10.1016/j.micromeso.2007.10.028.
109. Bonaccorsi, L.; Calabrese, L.; Freni, A.; Proverbio, E. Hydrothermal and microwave synthesis of SAPO (CHA) zeolites on aluminium foams for heat pumping applications. *Micropor. Mesopor. Mater.* **2013**, *167*, 30–37. https://doi.org/10.1016/j.micromeso.2012.06.006.
110. Ferone, C.; Esposito, S.; Pansini, M. Microwave assisted hydrothermal conversion of Ba-exchanged zeolite A into metastable paracelsian. *Micropor. Mesopor. Mater.* **2006**, *96*, 9–13. https://doi.org/10.1016/j.micromeso.2006.06.009.
111. Bonaccorsi, L.; Freni, A.; Proverbio, E.; Restuccia, G.; Russo, F. Zeolite coated copper foams for heat pumping applications. *Micropor. Mesopor. Mater.* **2006**, *91*, 7–14. https://doi.org/10.1016/j.micromeso.2005.10.045.
112. Taghavi, S.; Ghedini, E.; Menegazzo, F.; Mäki-Arvela, P.; Peurla, M.; Zendehdel, M.; Cruciani, G.; Di Michele, A.; Murzin, D.Y.; Signoretto, M. CuZSM-5@HMS Composite as an Efficient Micro-Mesoporous Catalyst for Conversion of Sugars into Levulinic Acid. *Catal. Today* **2022**, *390–391*, 146–161. https://doi.org/10.1016/j.cattod.2021.11.038.
113. Villa, C.; Rosa, R.; Corradi, A.; Leonelli, C. Microwaves-Mediated Preparation of Organoclays as Organic-/Bio-Inorganic Hybrid Materials. *Curr. Org. Chem.* **2011**, *15*, 284–295. https://doi.org/10.2174/138527211793979781.
114. Martina, K.; Tagliapietra, S.; Barge, A.; Cravotto, G. Combined Microwaves/Ultrasound, a Hybrid Technology. *Top. Curr. Chem*. **2016**, *374*, 79. https://doi.org/10.1007/s41061-016-0082-7.
115. Dalton, R.C.; Ahmad, I.; Clark, D.E. Combustion Synthesis Using Microwave Energy. *Ceram. Eng. Sci. Proc.* 1990, *11*(10), 1729–1742.
116. Roy, R.; Agrawal, D.; Cheng, J.; Gedevanishvili, S. Full Sintering of Powdered-Metal Bodies in a Microwave Field. *Nature* 1999, *399*, 668–670. https://doi.org/10.1038/21390.
117. Veronesi, P.; Rosa, R.; Colombini, E.; Leonelli, C.; Poli, G.; Casagrande, A. Microwave Assisted Combustion Synthesis of Non-Equilibrium Intermetallic Compounds. *J. Microw. Power Electromagn. Energ.* 2010, *44*(1), 46–56.

118. Rosa, R.; Veronesi, P.; Casagrande, A.; Leonelli, C. Microwave Ignition of the Combustion Synthesis of Aluminides and Field-Related Effects. *J. Alloys Compd.* 2016, *657*, 59–67. https://doi.org/10.1016/j.jallcom.2015.10.044.
119. Rosa, R.; Veronesi, P. Functionally Graded Materials. In *Functionally Graded Materials Obtained by Combustion Synthesis Techniques: A Review*; Reynolds, N.J., Ed.; Nova Science Publishers: New York, NY, USA, 2012; Chapter 2, pp. 93–122.
120. Colombini, E.; Rosa, R.; Veronesi, P.; Poli, G.; Leonelli, C. Microwave Ignited Combustion Synthesis as a Joining Technique for Dissimilar Materials: Modeling and Experimental Results. *Int. J. Self-Propag. High-Temp. Synth.* 2012, *21*(1), 25–31.
121. Poli, G.; Sola, R.; Veronesi, P. Microwave-Assisted Combustion Synthesis of NiAl Intermetallics in a Single Mode Applicator: Modeling and Optimisation. *Mater. Sci. Eng. A* 2006, *441*(1), 149–156. https://doi.org/10.1016/j.msea.2006.08.114.
122. Rosa, R.; Veronesi, P.; Leonelli, C. A Review on Combustion Synthesis Intensification by Means of Microwave Energy. *Chem. Eng. Process. Process Intensif.* 2013, *71*, 2–18. https://doi.org/10.1016/j.cep.2013.02.007.
123. Veronesi, P.; Leonelli, C.; Poli, G.; Casagrande, A. Enhanced Reactive NiAl Coatings by Microwave-Assisted SHS. *COMPEL* 2008, *27*(2), 491–499. https://doi.org/10.1108/03321640810847779.
124. Rosa, R.; et al. Alternative Sintering Processes: Microwave (MW)-Assisted Combustion Synthesis of Micrometric Metallic Powders for the Preparation of Intermetallic-Based Materials. In *European PM Conference Proceedings*; European Powder Metallurgy Association: Shrewsbury, UK, 2010; pp. 1–7.
125. Veronesi, P.; Colombini, E.; Rosa, R.; Leonelli, C.; Garuti, M. Microwave Processing of High Entropy Alloys: A Powder Metallurgy Approach. *Chem. Eng. Process. Process Intensif.* 2017, *122*, 397–403. https://doi.org/10.1016/j.cep.2017.02.016.
126. Trombi, L.; Cugini, F.; Rosa, R.; Amadè, N.S.; Chicco, S.; Solzi, M.; Veronesi, P. Rapid Microwave Synthesis of Magnetocaloric Ni–Mn–Sn Heusler Compounds. *Scr. Mater.* 2020, *176*, 63–66. https://doi.org/10.1016/j.scriptamat.2019.09.039.
127. Colombini, E.; Rosa, R.; Trombi, L.; Zadra, M.; Casagrande, A.; Veronesi, P. High Entropy Alloys Obtained by Field Assisted Powder Metallurgy Route: SPS and Microwave Heating. *Mater. Chem. Phys.* 2018, *210*, 78–86. https://doi.org/10.1016/j.matchemphys.2017.06.065.
128. Colombini, E.; Lassinantti Gualtieri, M.; Rosa, R.; Tarterini, F.; Zadra, M.; Casagrande, A.; Veronesi, P. SPS-Assisted Synthesis of SiCp Reinforced High Entropy Alloys: Reactivity of SiC and Effects of Pre-Mechanical Alloying and Post-Annealing Treatment. *Powder Metall.* 2018, *61*(1), 64–72. https://doi.org/10.1080/00325899.2017.1393162.
129. Colombini, E.; Gualtieri, M.L.; Pagetti, S.; Veronesi, P. Recycling of Spent Powders from Laser Powder Bed Fusion Processing of Inconel 625 for the Mechanical Synthesis of CoCrFeNiMoxNb0.4x (x = 0–0.1) Multi-Principal Element Alloys. In *EURO PM 2023 Conference Proceedings*; Curran Associates, Inc.: New York, NY, USA, 2024; pp. 126–133. ISBN 978-1-7138-8290-9.
130. Gasik, M. Microwave Processing of Materials in Metallurgy. *Theory Pract. Metall.* 2025, *1*, 10–15. https://doi.org/10.15802/tpm.1.2025.02.
131. Colombini, E.; Papalia, K.; Barozzi, S.; Perugi, F.; Veronesi, P. A Novel Microwave and Induction Heating Applicator for Metal Making: Design and Testing. *Metals* 2020, *10*, 676. https://doi.org/10.3390/met10050676.